

## Higgs Physics

---

### Christoph Englert

*SUPA, School of Physics and Astronomy, University of Glasgow, Glasgow G12 8QQ, UK*  
christoph.englert@glasgow.ac.uk

This is a write-up of lectures presented at TASI 2018, and provides a pedagogical introduction to the Higgs mechanism in the Standard Model as well its phenomenological implications at hadron colliders. Particular emphasis is given to search and analysis strategies for generic beyond the Standard Model extensions.

*Theoretical Advanced Study Institute Summer School 2018 'Theory in an Era of Data' (TASI2018)*  
*4 - 29 June, 2018*  
*Boulder, Colorado*

## 1. Introduction

The Higgs discovery in 2012 marks a milestone of particle physics in two major ways. Firstly, it is the spectacular verification of a theoretical concept that was chiefly proposed in 1964 independently by Higgs, Brout and Englert [1–3]. Secondly, it turns particle physics post 2012 into a leap into the unknown. It is not uncommon that the successful experimental verification of a theoretical idea takes time. However, the latter point certainly provides a new backdrop to particle physics that had been dominated by theoretical consistency arguments. These led to the observation of the Higgs boson in the vicinity where it was expected, with predictions firmly based on the application of perturbative renormalizable field theory.

The Standard Model of Particle Physics (SM), which crucially depends on the Higgs mechanism can therefore be rightly considered as the pinnacle of perturbative Quantum Field Theory (QFT). As a matter of fact, the observation of massive electroweak gauge bosons that lie at the heart of Fermi’s theory [4] and which were later directly observed at UA1/UA2, left little room for theoretical concepts other than a perturbative Higgs mechanism as proposed by Higgs and others. As ’t Hooft puts it in [5]: The Higgs mechanism had to be right as there was no viable or elegant alternative. Sure enough, there were other contenders on the market such as Technicolor etc., but it is fair to say that these intrinsically non-perturbative scenarios created more problems than provided solutions. This statement was sharpened over the years leading up to the Higgs discovery: if we would like to have a theoretically consistent *perturbative* formulation of the electroweak scale, a Higgs mechanism in some manifestation responsible for spontaneous breaking of electroweak symmetry is the only viable option [6–8].

In this sense, the Higgs discovery also concludes an endeavour to understand symmetry in particle physics. Starting with (non-)abelian gauge theories which consistently describe massless force mediators when realized linearly, Higgs and others [1–3, 9] extended this to non-linear realizations of gauge+scalar systems that are compatible with a non-trivial vacuum to describe massive gauge bosons. Coleman and Mandula showed in [10] that internal and external (Poincaré) symmetries can only be trivially combined in realistic field theories<sup>1</sup>. Non-linear realization of gauge symmetries therefore extend the linear transformations along these lines when combined with the irreducible representations (“particles”) of the Lorentz group that we observe.

So what’s next? The only objective answer at this point in time is: we do not know. As the SM is complete, we do not have another QFT consistency argument at our disposal. Furthermore, the (arguably early) investigation of the Higgs boson and its interactions with known matter shows no tension with the SM expectation. This seems to suggest that Higgs physics is old news - but this would be a dramatic and unrealistic exaggeration. Firstly, we have just started to explore the mechanism of electroweak symmetry breaking, and there is still plenty of space for the SM to be ruled out along these lines. Secondly, the Higgs has not been observed in a beyond the SM vacuum but provides a tremendous opportunity to resolve some of the SM’s other shortcomings, especially when we consider the SM in the context of cosmological facts such as an apparent matter–anti-matter asymmetry. Furthermore, by exhausting the symmetry possibilities offered by the Coleman-Mandula theorem, the Higgs boson creates its own 21st century version of the Ultra-

---

<sup>1</sup>Supersymmetry is an exception that we will not be dealing with in these lectures.

violet Catastrophe (the Hierarchy Problem), whose solution has been the driving force for model building for beyond the SM (BSM) physics.

In these lectures we will cover the basics of (electroweak) symmetry breaking as well as a primer on Higgs phenomenology. We will show avenues how we can connect the SM Higgs sector to BSM physics and discuss some of the phenomenological implications. More specific lectures on concrete BSM extensions have been presented by other lecturers at this school and their notes will be more detailed on these parts. I also encourage you to have a look at notes from previous years, in particular Sally Dawson's notes [11]. A more comprehensive overview of the phenomenological status of Higgs physics can be found in [12].

## 2. Electroweak Symmetry Breaking

### 2.1 Abelian Higgs Model

Gauge theories are the foundation of modern physics. A direct implication of gauge theories is a massless force-mediator. This is particularly highlighted by the example of Quantum Electrodynamics (QED) which describes the interaction between electrically charged fermions and a vector field (the photon field  $A^\mu$ ). QED in its classical formulation starts with Maxwell's equations in relativistic notation using the field strength tensor  $F^{\mu\nu}$

$$\partial_\mu F^{\mu\nu} = j^\nu, \quad \text{where} \quad F^{\mu\nu} = \partial^\mu A^\nu - \partial^\nu A^\mu, \quad (2.1)$$

where we have defined vector fields

$$A^\mu = \begin{pmatrix} \phi \\ \vec{A} \end{pmatrix}, \quad j^\mu = \begin{pmatrix} \rho \\ \vec{j} \end{pmatrix} \quad (2.2)$$

that collect the scalar and vector potentials as well as charge and current densities from Electrodynamics. From these  $\vec{E}, \vec{B}$  can be obtained via

$$\vec{E} = -\vec{\nabla}\phi - \frac{\partial\vec{A}}{\partial t}, \quad \vec{B} = \nabla \times \vec{A}. \quad (2.3)$$

$j^\nu$  is a conserved current, i.e. satisfying  $\partial_\nu j^\nu = 0$  because  $F^{\mu\nu}$  is anti-symmetric for  $\mu \leftrightarrow \nu$ . The remaining 4 equations are

$$\partial_\mu \tilde{F}^{\mu\nu} = 0, \quad \text{where} \quad \tilde{F}^{\mu\nu} = \frac{1}{2} \epsilon^{\mu\nu\alpha\beta} F_{\alpha\beta}, \quad (2.4)$$

where we have defined the dual field strength tensor  $\tilde{F}^{\mu\nu}$ . We have  $\tilde{\tilde{F}} = F$ , which is equivalent to identifying  $\vec{D}, \vec{E}$ , and  $\vec{H}, \vec{B}$ .

Maxwell's equations can be derived from the Lagrangian

$$\mathcal{L} = \mathcal{L}_{\text{em}} + \mathcal{L}_{\text{int}}, \quad \mathcal{L}_{\text{em}} = -\frac{1}{4} F^{\mu\nu} F_{\mu\nu}, \quad \mathcal{L}_{\text{int}} = -j^\mu A_\mu, \quad (2.5)$$

by applying Euler-Lagrange equations

$$\partial_\mu \frac{\partial \mathcal{L}}{\partial(\partial_\mu A_\nu)} - \frac{\partial \mathcal{L}}{\partial A_\nu} = -\partial_\mu F^{\mu\nu} + j^\nu = 0. \quad (2.6)$$

The Dirac equation for a spinor  $\psi$  or for  $\bar{\psi} = \psi^\dagger \gamma^0$  can be derived from the Lagrangian

$$\mathcal{L}_{\text{Dirac}} = \bar{\psi}(i\gamma^\mu \partial_\mu - m)\psi. \quad (2.7)$$

The starting point for the QED Lagrangian is then the sum of  $\mathcal{L}_{\text{em}}$  and  $\mathcal{L}_{\text{Dirac}}$ . However, in order to make the theory describe interactions, we must include a term which couples  $A^\mu$  to  $\psi$  and  $\bar{\psi}$ . If we wish Maxwell's equation to be valid, this term has to be of the form  $\mathcal{L}_{\text{int}} = -j^\mu A_\mu$ , with  $j^\mu$  a conserved vector current. We can show that  $\bar{\psi}\gamma^\mu\psi$  is conserved using Noether's theorem and  $\psi$ 's phase freedom. Therefore, a good candidate for the electromagnetic current describing an electron of charge  $-e$  is

$$j^\mu = -e \bar{\psi} \gamma^\mu \psi. \quad (2.8)$$

At this stage  $-e$  is just a proportionality constant. But one can see that it indeed needs to be the electric charge from calculating the non-relativistic Coulomb potential that arises as a limit. Using the above current, we obtain:

$$\mathcal{L} = \mathcal{L}_{\text{em}} + \mathcal{L}_{\text{Dirac}} + \mathcal{L}_{\text{int}} = -\frac{1}{4}F^{\mu\nu}F_{\mu\nu} + \bar{\psi}(i\not{\partial} - m)\psi + e\bar{\psi}\gamma^\mu\psi A_\mu. \quad (2.9)$$

Notice that  $\mathcal{L}$  is invariant with respect to the ‘‘gauge’’  $U(1)$  transformations

$$\psi(x) \mapsto \psi'(x) = e^{-ie\alpha(x)}\psi(x), \quad A_\mu(x) \mapsto A'_\mu(x) = A_\mu(x) + \partial_\mu\alpha(x). \quad (2.10)$$

Notice also that the addition of the interaction term  $\mathcal{L}_{\text{int}}$  is equivalent to the replacement

$$\partial_\mu \rightarrow D_\mu = \partial_\mu - ieA_\mu. \quad (2.11)$$

This prescription is known as ‘‘minimal coupling’’ or ‘‘covariant derivative’’ and automatically ensures that the Lagrangian is gauge invariant. The use of gauge invariance to introduce interactions is a key principle of particle physics. In total, we have

$$\mathcal{L} = -\frac{1}{4}F^{\mu\nu}F_{\mu\nu} + \bar{\psi}[i\gamma^\mu(\partial_\mu + ieA_\mu)]\psi. \quad (2.12)$$

The fact that  $\mathcal{L}$  is invariant under the gauge transformations in Eq. (2.10) means that  $A^\mu$  contains unphysical degrees of freedom. This is clear in view of the fact that a massless vector field contains two physical polarisations, whereas  $A^\mu$  has four degrees of freedom. In order to eliminate this degeneracy, a ‘‘gauge-fixing’’ condition is imposed. A possible choice of a gauge condition is the so-called Coulomb gauge, in which  $\nabla \cdot \mathbf{A} = 0$ . Although this condition eliminates the two additional degrees of freedom, it breaks Lorentz covariance. A common choice that preserves Lorentz covariance is the Lorentz gauge

$$\partial_\mu A^\mu = 0. \quad (2.13)$$

This corresponds to choosing the gauge parameter  $\alpha$  such that  $\square\alpha = -\partial_\mu A^\mu$  above. In this gauge, the Maxwell equations become  $\square A^\nu = 0$ . The Lorentz gauge condition reduces the number of degrees of freedom in  $A$  from four to three. Even now though  $A^\mu$  is not unique. A transformation of the form

$$A_\mu \rightarrow A'_\mu = A_\mu + \partial_\mu\chi, \quad \square\chi = 0, \quad (2.14)$$

will also leave the Lagrangian unchanged. At classical level we can eliminate the extra polarisation “by hand”, but at quantum level this cannot be done without giving up covariant canonical commutation rules. The way out, which we can only summarize<sup>2</sup>, is to add a gauge-fixing Lagrangian  $\mathcal{L}_{\text{gf}}$ , so that the full QED Lagrangian becomes

$$\mathcal{L}_{\text{QED}} = \mathcal{L}_{\text{em}} + \mathcal{L}_{\text{Dirac}} + \mathcal{L}_{\text{int}} + \mathcal{L}_{\text{gf}}, \quad \mathcal{L}_{\text{gf}} = -\frac{1}{2\xi}(\partial_\mu A^\mu)^2. \quad (2.15)$$

The transformation of Eq. (2.10) shows that adding a mass term to the QED Lagrangian  $\sim m_A^2 A^\mu A_\mu$  will explicitly break the  $U(1)$  gauge symmetry. One can show that violating gauge symmetry typically introduces a bad high-energy behaviour of the resulting theory and we will no longer deal with a probabilistically well-behaved theory.

Now we face a problem: gauge theories are extremely successful concepts. QED and Quantum Chromodynamics (QCD) agree with measurements over many orders of magnitude. Yet, the  $W$  and  $Z$  bosons have a large mass of 80.42 GeV and 91.18 GeV, respectively. How can we match up theoretical necessity with experimental facts?

Peter Higgs and others came up with a cunning idea to introduce mass terms for gauge bosons in a dynamical way. The argument is heuristically outlined in Fig. 1. Starting with a free and massless theory, where the  $U(1)$  gauge boson propagator essentially behaves like  $\sim ip^{-2}$  we can switch on some interaction with a constant background field with a strength  $-i\Sigma = ie^2\langle\phi\rangle^2$ . Here  $e$  is again the electric coupling constant. Dyson-resumming the 1 particle irreducible (1PI) interaction insertions, together with the geometric series gives us

$$\begin{aligned} & \underbrace{\frac{i}{p^2}}_{\text{free theory}} + \underbrace{\frac{i}{p^2}(-i\Sigma)\frac{i}{p^2}}_{\text{1PI}} + \underbrace{\frac{i}{p^2}(-i\Sigma)\frac{i}{p^2}(-i\Sigma)\frac{i}{p^2}}_{(\text{1PI})^2} + \dots \\ &= \frac{i}{p^2} \left( 1 + \frac{\Sigma}{p^2} + \left[ \frac{\Sigma}{p^2} \right]^2 + \left[ \frac{\Sigma}{p^2} \right]^3 + \dots \right) \\ &= \frac{i}{p^2} \sum_{i=0}^{\infty} \left[ \frac{\Sigma}{p^2} \right]^i = \frac{i}{p^2} \left( 1 - \frac{\Sigma}{p^2} \right)^{-1} = \frac{i}{p^2 - e^2\langle\phi\rangle^2}. \end{aligned} \quad (2.16)$$

This means that in the interacting theory, the mass pole of the  $A$  field has shifted to  $p^2 = m_A^2 = e^2\langle\phi\rangle^2$ . As we are now dealing with a massive vector boson, we also pick up an additional longitudinal polarisation of the gauge boson which behaves for large four-momenta as

$$\varepsilon^\mu(k) \simeq \frac{k^\mu}{m_A}. \quad (2.17)$$

It is exactly the behaviour of these longitudinal polarisations that causes problems at large energies if we break electroweak symmetry by hand.

<sup>2</sup>The alert reader might highlight that the whole procedure of gauge-fixing ultimately breaks gauge-invariance. This is true, however, so far, we have cared little about whether we understand the theory as a classical or quantum one. Without gauge-fixing we would not be able to find the inverse of the gauge boson operator (the propagator) as the former has eigenvalues zero. Using the restriction of Lorentz-gauge lifted from a classical statement to a statement that is compatible with our QFT Fock space makes things a little more complicated but ultimately clarifies this conundrum. While the origin of the gauge-fixing term in the Lagrangian is most transparent in the path-integral formalism, the alternative approach known as the *Gupta-Bleuler formalism* is worth checking out.



**Figure 1:** The full propagator on the left side is obtained by Dyson-resumming all 1PI insertions denoted by the black circles ( $= -i\Sigma$ ).

Of course this discussion was a bit leading, but it alludes to the possibility of including mass terms through gauge dynamics. As we would like to furnish a vacuum expectation value (vev) without breaking Lorentz covariance, we are left with scalar fields as viable candidates to achieve this. So let us introduce a complex scalar with gauge interactions as described above

$$\mathcal{L} = D_\mu \phi^\dagger D^\mu \phi - V(\phi) + \mathcal{L}_{\text{em}}. \quad (2.18)$$

The potential is only constrained by gauge invariance which limits allowed terms to the form  $\sim \phi^\dagger \phi$ , and possibly renormalizability arguments, which cut off interaction terms at the dimension 4 level. This gives

$$V(\phi) = \mu^2 \phi^\dagger \phi + \lambda (\phi^\dagger \phi)^2. \quad (2.19)$$

To find the classical minimum of the theory we need look for the minimum of  $V$

$$V'(|\phi|^2) = 0 \quad \implies \quad |\phi|^2 = -\frac{\mu^2}{2\lambda} \quad (2.20)$$

which leaves to choices

- $\mu^2 > 0$ : In this case there is only the trivial minimum  $|\phi| = 0$ . For this choice the Lagrangian of Eq. (2.18) would be nothing else but a massive, self-interacting scalar that we have coupled to Electrodynamics. While this is a perfectly viable field theory, it is not really what we are after.
- $\mu^2 < 0$ : The scalar field looks like a tachyon, which signals an instability. Indeed  $|\phi| = 0$  is a local maximum and  $|\phi|^2 = v^2/2$  with  $v = -\mu^2/\lambda$  is a minimum.

The second option looks much more interesting. As we would like to eventually do perturbation theory around the new vacuum that is characterized by a vev  $\langle \phi \rangle = v/\sqrt{2}$ , we can write the scalar field as

$$\phi(x) = \frac{1}{\sqrt{2}} e^{i\chi(x)/v} (v + h(x)) \quad (2.21)$$

around the minimum. Plugging this back into the original Lagrangian, we obtain

$$\mathcal{L} = -\frac{1}{4} F^{\mu\nu} F_{\mu\nu} + \frac{e^2 v^2}{2} A_\mu A^\mu \quad (2.22)$$

$$+ \frac{1}{2} \partial_\mu h \partial^\mu h + \mu^2 h^2 + e^2 v A_\mu A^\mu h + \frac{1}{2} e^2 A_\mu A^\mu h^2 \quad (2.23)$$

$$+ \frac{1}{2} \partial_\mu \chi \partial^\mu \chi - ev A_\mu \partial^\mu \chi + \dots, \quad (2.24)$$

where we have suppressed some interactions for the time being.

This shows that we have achieved what we set out to achieve with a simple version of a general strategy that is referred to as ‘‘Higgs mechanism’’. The first line Eq. (2.22) shows that we indeed

have generated a mass term for our gauge field. Its mass is not arbitrary, but is related to the interaction strength as well as the order parameter  $m_A = ev$ ;  $v$  determines whether symmetry is “broken” or intact.

The second line is a prediction of this mechanism: There is a scalar boson with mass  $m_h^2 = 2\mu^2$ , whose coupling to the massive gauge boson follows the distinctive pattern  $\sim [\text{coupling}] \times [\text{boson mass}] = em_A$ . Quartic interactions  $\sim A^2 h^2$  are gauge-interactions.

There is also an additional massless (Goldstone) scalar  $\chi$ , which is special: it mixes with the gauge field Eq. (2.24), proportional to the obtained mass of the vector field. This last term is crucial to maintain gauge-invariance as is explicit in the original Lagrangian Eq. (2.18). This mixing becomes more relevant for high-energies  $\sim m_A k^\mu$ , exactly where we would anticipate a problem following our remarks around Eq. (2.17). This is an important result of the Higgs mechanism: gauge bosons at large momenta effectively behave like derivatively-coupled scalar fields. As there are no issues with the latter at high energies, theories that implement a Higgs mechanism along our abelian Higgs example above will maintain a good high energy behaviour. In fact, gauge symmetry is not broken at all, but realized non-linearly between  $A_\mu, \chi, h$  in such a way that gauge symmetry is compatible with a non-zero vev  $\sim v$  that also manifests itself as a gauge boson mass.

As we would like to apply perturbation theory, the mixing  $\sim A_\mu \partial^\mu \chi$  is unwanted. We can get rid of it by adding a modified gauge-fixing term ( $R_\xi$  gauge-fixing [13])

$$\begin{aligned} \mathcal{L}_{\text{gf},\chi} &= -\frac{1}{2\xi} (\partial_\mu A^\mu + \xi m_A \chi)^2 \\ &= -\frac{1}{2\xi} (\partial_\mu A^\mu)^2 - m_A \partial_\mu A^\mu \chi - \frac{(m_A \sqrt{\xi})^2}{2} \chi^2. \end{aligned} \quad (2.25)$$

Partial integration of the second term exactly cancels the mixing term in Eq. (2.24). We recover the original gauge-fixing term and introduce a fixing-dependent mass term of  $\chi$ .  $\xi$  is a free parameter of this procedure and we need to ensure that our final results do not depend on our particular choice. This can be formally proven and relies on symmetries of the gauge-fixed Lagrangian (BRST invariance [14–17]) and is the formal justification of treating gauge symmetry breaking completely analogous to global symmetry breaking (with, however, very different quantum implications).

Using standard techniques we can derive the expressions for the  $A_\mu$  and  $\chi$  propagators in this theory

$$\Delta_{\mu\nu}^A(p^2) = -\frac{i}{p^2 - m_A^2} \left( g_{\mu\nu} - \frac{(1 - \xi)p_\mu p_\nu}{p^2 - \xi m_A^2} \right), \quad (2.26)$$

$$\Delta^\chi(p^2) = \frac{i}{p^2 - \xi m_A^2}. \quad (2.27)$$

Again we see that the  $A^\mu$  propagator has a non-trivial dependence on  $\sim p_\mu p_\nu$  which can be dangerous when the gauge fields run in loops and which could destroy power-counting arguments for the convergence of Feynman integrals. This would have bad consequences for the theory’s renormalizability. However, we can see that these terms are gauge-dependent in the context of the Higgs mechanism and choosing, e.g.,  $\xi = 1$  (so-called “Feynman gauge”) removes this behaviour altogether at the price of an additional propagating scalar degree freedom with mass  $m_A$ .

The standard approach to computations of loop diagrams and their reduction to a basis of scalar 1-loop integrals works for general  $\xi$  [18]. The independence of the final physical result of  $\xi$  is a strong consistency check for higher order computations. Electroweak corrections are typically small for energies in the vicinity of the electroweak scale and many processes are sufficiently described by the leading order approximation in the electromagnetic coupling constant. If we are not interested in higher-order effects, then bookkeeping gauge-dependencies can be tedious and we can simplify our lives considerably by approaching the limit  $\xi \rightarrow \infty$ , so-called ‘‘unitary gauge’’ where the scalar propagator vanishes (the would-be Goldstone boson decouples from the theory). Then

$$\Delta_{\mu\nu}^A(p^2) = -\frac{i}{p^2 - m_A^2} \left( g_{\mu\nu} - \frac{p_\mu p_\nu}{m_A^2} \right). \quad (2.28)$$

Unitary gauge also means rotating away the Goldstone bosons in Eq. (2.21) through an appropriate gauge transformation  $e\alpha = \xi/v$ . In unitary gauge, as we have removed the  $\chi$  fields that were crucial for the realization of gauge-symmetry, we have lost gauge-invariance. However, we have lost it in a controlled way, by implicitly choosing  $\xi m_A \gg m_A$ , so physics that is sensitive to the mass scale  $m_A$  will not be affected by this choice and we can formally decouple the threshold necessary for gauge-invariance using  $\xi \rightarrow \infty$ . There is no free lunch: this simplification is not admissible for quantum effects as virtual corrections explore arbitrarily large energy scales and will resolve this shortcoming of the simplified theory in the UV.

## 2.2 Weinberg-Salam Model

We are now in the position to generalize the abelian Higgs model of the previous section to the electroweak Standard Model [19–22]. The strategy is entirely the same as in the abelian case, except that we consider are more complex gauge group  $SU(2)_L \times U(1)_Y$

$$\mathcal{L} = -\frac{1}{4} W_{\mu\nu}^a W^{a\mu\nu} - \frac{1}{4} B^{\mu\nu} B_{\mu\nu} \quad (2.29)$$

where the  $SU(2)_L$  and  $U(1)_Y$  field strengths are given by

$$W_{\mu\nu}^a = \partial_\mu W_\nu^a - \partial_\nu W_\mu^a + g \varepsilon^{abc} W_\mu^b W_\nu^c \quad (2.30)$$

$$B_{\mu\nu} = \partial_\mu B_\nu - \partial_\nu B_\mu. \quad (2.31)$$

$g$  denotes the  $SU(2)_L$  gauge coupling constant and we will refer to the  $U(1)_Y$  hypercharge coupling as  $g'$ .  $\varepsilon$  is the Levi-Civita tensor in three dimensions, i.e. the structure constants of the  $su(2)$  Lie algebra ( $a, b, c = 1, 2, 3$ ). The covariant derivative is

$$D_\mu = \partial_\mu - ig t^a W_\mu^a - ig' Y B_\mu, \quad (2.32)$$

where  $t^a = \sigma^a/2$  are the generators of  $su(2)$ . Again we introduce a scalar  $\Phi$ , the Higgs field, transforming as a  $\mathbf{2}_{1/2}$  under  $SU(2)_L \times U(1)_Y$  with potential

$$V(\Phi) = \mu^2 \Phi^\dagger \Phi + \lambda (\Phi^\dagger \Phi)^2. \quad (2.33)$$

Just like in the  $U(1)$  model of the previous section this leads to a non-trivial vacuum for  $\mu^2 < 0$ , which again only constrains the modulus of  $\Phi$  to be  $v/\sqrt{2}$ . To perform perturbation theory, we

have to make a choice in which  $SU(2)$  direction we would like to align this vev. Note that this choice is completely arbitrary, and physics will not depend on this choice as any other choice can be obtained by a suitable  $SU(2)_L$  transformation. This is again related to  $R_\xi$  gauge-fixing that we will not discuss in its full glory for the Weinberg-Salam model (for a more detailed treatment see Refs. [18, 23]).

We know that the mass terms will arise from the Higgs field's kinetic term

$$\mathcal{L}_{\text{Higgs}} \supset D_\mu \Phi^\dagger D^\mu \Phi \supset \frac{v^2}{8} (\vec{W}, B)^\mu \begin{pmatrix} g^2 & 0 & 0 & 0 \\ 0 & g^2 & 0 & 0 \\ 0 & 0 & g^2 & gg' \\ 0 & 0 & gg' & g'^2 \end{pmatrix} \begin{pmatrix} \vec{W} \\ B \end{pmatrix}^\mu. \quad (2.34)$$

To find the physical mass basis we only need to diagonalize the  $2 \times 2$  subspace that mixes  $W^3$  and  $B$ . The related two-dimensional isometry is parametrized by a single angle  $\theta_w$  (the Weinberg angle). The mass<sup>2</sup> eigenvalues for the real fields are

$$m_{W^1}^2 = m_{W^2}^2 = \frac{g^2 v^2}{4} \quad (2.35)$$

$$m_Z^2 = \frac{(g^2 + g'^2) v^2}{4} \quad (2.36)$$

$$m_A^2 = 0 \quad (2.37)$$

and the Weinberg angle is given by

$$\cos^2 \theta_w = \frac{g^2}{g^2 + g'^2}. \quad (2.38)$$

This rotates the Lagrangian fields into mass eigenstates

$$\begin{pmatrix} Z \\ A \end{pmatrix}^\mu = \begin{pmatrix} \cos \theta_w & -\sin \theta_w \\ \sin \theta_w & \cos \theta_w \end{pmatrix} \begin{pmatrix} W^3 \\ B \end{pmatrix}^\mu. \quad (2.39)$$

The vanishing mass for the  $A$  field (already apparent from the vanishing determinant of the mass mixing matrix) signalizes an unbroken  $U(1)$  gauge symmetry associated with the direction

$$Q = t^3 + Y \quad (2.40)$$

that we identify with QED with coupling strength

$$e = \frac{gg'}{\sqrt{g^2 + g'^2}} = g' \cos \theta_w = g \sin \theta_w. \quad (2.41)$$

It is advisable to make unbroken symmetries apparent.  $W^{1,2}$  are transforming under the adjoint representation of  $su(2)$  and QED becomes explicit when we define

$$W_\mu^\pm = \frac{1}{\sqrt{2}} (W_\mu^1 \mp W_\mu^2) \quad (2.42)$$

which are eigenstates of  $Q$  as  $Y(W^{1,2}) = 0$ . With this, the gauge mass terms become

$$\mathcal{L}_{\text{Higgs}} \supset \underbrace{\frac{g^2 v^2}{4} W_\mu^+ W^{-\mu}}_{=m_W^2} + \underbrace{\frac{(g^2 + g'^2)v^2}{8} Z^\mu Z_\mu}_{=m_Z^2/2}. \quad (2.43)$$

Interestingly enough we have

$$\frac{m_W^2}{m_Z^2} = \frac{g^2}{g^2 + g'^2} = \cos^2 \theta_w. \quad (2.44)$$

This is entirely unexpected as the characteristic angle of an isometry is typically not correlated with the eigenvalues of the matrix that it diagonalizes. This is even more relevant as the coupling relation can be determined from the gauge interactions of the  $W$  and  $Z$  bosons with fermions (analogous to Eq. (2.12)) and compared to the masses extracted from resonance searches at experiments. A prediction of the Weinberg-Salam model is that these measurements should be compatible with each other, and in fact they are. The reason for this relation, which has been verified experimentally to very high precision (see later) is that the Higgs sector as we introduced it has a bigger (accidental) symmetry than expected. It is based on the fact the  $\mathbf{2}$  of  $SU(2)$  is symplectic:  $\mathbf{2} \sim \bar{\mathbf{2}}$ . We can straightforwardly check that if  $\Phi \mapsto U\Phi$  for  $U \in SU(2)$ , also

$$\Phi^c = i\sigma^2 \Phi^* \mapsto U\Phi^c. \quad (2.45)$$

Instead of working with  $\Phi$  we could look at any normalized superposition of  $\Phi, \Phi^c$ . To make this explicit we consider the bi-doublet

$$\mathcal{H} = (\Phi^c, \Phi) \quad (2.46)$$

and obtain

$$\Phi^\dagger \Phi = \frac{1}{2} \text{Tr}(\mathcal{H}^\dagger \mathcal{H}). \quad (2.47)$$

This implies that  $V(\Phi) = V(\Phi^\dagger \Phi)$  is only a function of  $\text{Tr}(\mathcal{H}^\dagger \mathcal{H})$ . A similar result holds for the kinetic term (only violated by the different hypercharge assignments). The trace is invariant under the bigger symmetry  $SU(2)_L \times SU(2)_R$

$$\mathcal{H} \mapsto U_L \mathcal{H} U_R^\dagger. \quad (2.48)$$

When the Higgs field obtains its vev, the bi-doublet becomes

$$\langle \mathcal{H} \rangle = \frac{v}{\sqrt{2}} \mathbf{1}, \quad (2.49)$$

which breaks  $SU(2)_L \times SU(2)_R \rightarrow SU(2)_D$  as the vacuum is still invariant under  $U_L = U_R$ . This means that all mass eigenvalues have to be identical in order for  $SU(2)_D$  to be a good symmetry before rotating to the mass eigenstates. This is why we see a correlation of  $m_W = m_Z \cos \theta_w$ .

$SU(2)_R$  is not exact as hypercharge gauging can be embedded along the  $t_R^3$  direction. Gauging a subgroup is tantamount to explicit breaking and we can therefore expect corrections to Eq. (2.44) proportional to  $\sim g'$  from Higgs contributions (see later). As this is a relatively small coupling and the corrections are logarithmic, these effects are not too large for moderate Higgs masses.

Turning to fermions, we can re-use our  $\Phi^c$  to obtain masses for up- and down-like fermions in a gauge-invariant way. Using the same Higgs field for both up- and down-type fermions is specific

to the SM, and typically relaxed in, e.g. two Higgs doublet models. We understand fermions as spinorial representations of the Lorentz group (or its even subalgebra). With the help of the  $\gamma^\mu$  matrices we can define left- and right-handed chirality projectors

$$P_{L,R} = \frac{1}{2}(1 \mp \gamma_5), \quad \gamma_5 = i\gamma^0\gamma^1\gamma^2\gamma^3. \quad (2.50)$$

with

$$\{\gamma^\mu, \gamma_5\} = 0, \quad (\gamma^5)^2 = 1. \quad (2.51)$$

It is easy to see that

$$P_{L,R}^2 = P_{L,R}, \quad P_{L,R}P_{R,L} = 0, \quad (2.52)$$

which shows that these objects are indeed projectors. The  $\gamma_5$  can be used to extend the Lorentz symmetry to the 5d case, which is relevant in theories with extra dimensions. Such a theory, however, will have no a-priori notion of chirality. Given that the Lorentz symmetry generators are given by  $\sim [\gamma^\mu, \gamma^\nu]$  it is straightforward to see that chirality will not change under Lorentz transformations and we are therefore allowed to assign different gauge quantum numbers to right- and left-handed fields (in fact the Weyl spinors  $\psi_{L,R}$  that we obtain from the Dirac spinor  $\psi$  using  $P_{L,R}$  are the relevant irreducible spinor representations of the Lorentz group). Fermi's theory then tells us that the coupling structure should be

$$Q_L = \begin{pmatrix} u_L \\ d_L \end{pmatrix} \quad \mathbf{2}_{1/6} \quad L_L = \begin{pmatrix} \nu_L \\ e_L \end{pmatrix} \quad \mathbf{2}_{-1/2} \quad (2.53)$$

$$u_R \quad \mathbf{1}_{2/3} \quad e_R \quad \mathbf{1}_{-1} \quad (2.54)$$

$$d_R \quad \mathbf{1}_{-1/3} \quad (2.55)$$

under  $SU(2)_L \times U(1)_Y$ , suppressing QCD  $SU(3)_c$ . With these assignments we can see that we get indeed the right electric charges, but also all perturbative anomalies cancel, which is a non-trivial consistency requirement for chiral gauge theories. The different hypercharge assignments to obtain the correct QED charge, however, tell us that we cannot write down fermion mass terms directly or with  $\Phi$  alone. For down-type masses, we can write down the gauge-invariant operator

$$\mathcal{L}_d = -y_d \bar{Q}_L \Phi d_R + \text{h.c.} \xrightarrow{\Phi \rightarrow \langle \Phi \rangle} -\frac{y_d v}{\sqrt{2}} \bar{d}_L d_R + \text{h.c.}, \quad (2.56)$$

where  $y_d$  is a dimensionless Yukawa coupling that allows us to obtain a mass term  $m_d = y_d v / \sqrt{2}$ . For up-type masses we can employ  $\Phi^c$

$$\mathcal{L}_u = -y_u \bar{Q}_L \Phi^c u_R + \text{h.c.} \xrightarrow{\Phi \rightarrow \langle \Phi \rangle} -\frac{y_u v}{\sqrt{2}} \bar{u}_L u_R + \text{h.c.}, \quad (2.57)$$

giving an up-type mass  $m_u = y_u v / \sqrt{2}$ .

In this discussion we have ignored the fact that the Yukawa couplings are indeed  $3 \times 3$  matrices in generation space. This means that the mass terms that are obtained through  $\Phi \rightarrow \langle \Phi \rangle$  are not necessarily diagonal but can be diagonalized with bi-unitary transformations that act on the chiral fermions  $Q_L, u_R, d_R$ . As  $u_L, d_L$  are contained in the same doublet the only visible effect

of this transformation is in the charged-current interactions of the fermions  $\sim \bar{u}_L \gamma^\mu d_L$  with the  $W$  bosons, which gives rise to the Cabibbo-Kobayashi-Maskawa matrix. All other neutral currents are unaffected by rotating to the fermion mass-eigenstates.

We are now ready to fix the theory's input parameters. The decay of the muon, Fig. 2 is particularly suited to fix the electroweak vacuum expectation value. In parallel, it is a prime example of applying effective field theory techniques (more later). As the mass of the muon is much smaller than

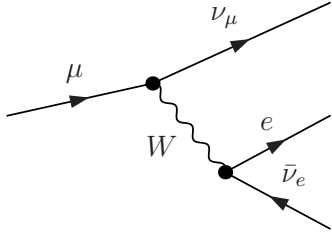


**Figure 2:** Muon decay Feynman diagram.

$m_W$ , we can expand the relevant part of the  $W$  propagator

$$\frac{1}{t - m_W^2} = -\frac{1}{m_W^2} - \frac{t}{m_W^4} + \dots \quad (2.58)$$

with (assuming massless neutrinos)

$$t = (p(\nu_\mu) - p(\mu))^2 = m_\mu(m_\mu - 2E_\nu). \quad (2.59)$$

So  $t < m_\mu^2$  and the second term in the Taylor expansion only gives rise to a  $\sim 10^{-6}$  correction. Neglecting these contributions, the muon decay is parametrized by a four-fermion interaction with strength  $G_\mu = 1.16638 \times 10^{-5} \text{ GeV}^{-2}$ , which is experimentally determined very accurately. The matching calculation  $\sim m_W^{-2}$  then allows us to find

$$\frac{G_\mu}{\sqrt{2}} = \frac{g^2}{8m_W^2} = \frac{1}{2v^2} \implies v = (\sqrt{2}G_\mu)^{-1/2} \simeq 246 \text{ GeV}. \quad (2.60)$$

To fix the remaining parameters of the gauge boson sector, we need the Weinberg angle

$$\sin^2 \theta_w \simeq 0.23 \quad (2.61)$$

and the  $W$  mass

$$m_W \simeq 80.42 \text{ GeV}. \quad (2.62)$$

With these parameters (referred to as  $G_\mu$ -scheme) we can compute all remaining parameters, in particular the electroweak coupling

$$e^2 = 4\sqrt{2}G_\mu m_W^2 \sin^2 \theta_w. \quad (2.63)$$

Alternatively one can define the so-called  $\alpha$ -scheme that uses the fine structure constant as input. These choices become relevant when one considers electroweak corrections, we will have a closer look at this below.

After the Higgs boson discovery giving

$$m_h^2 = 2v^2 \lambda \simeq (125 \text{ GeV})^2 \quad (2.64)$$

these parameters are also enough to fully specify the Higgs sector, i.e. in unitary gauge

$$V(h) = \frac{m_h^2}{2} h^2 + \frac{m_h^2}{2v} h^3 + \frac{m_h^2}{v^2} h^4. \quad (2.65)$$

As  $h$  fluctuates around the vev we can directly infer the relevant Higgs interactions in unitary gauge by making the replacement  $v \rightarrow v + h$ , which gives  $W$ -Higgs interactions

$$m_W^2 W^{+\mu} W_\mu^- \rightarrow m_W^2 W^{+\mu} W_\mu^- + g m_W h W^{+\mu} W_\mu^- + \frac{g^2}{2} W^{+\mu} W_\mu^- h^2. \quad (2.66)$$

In particular the form of the trilinear couplings is a tell-tale story of the Higgs mechanism. Gauge-boson masses appeared from the Higgs kinetic term in the presence of a vev, hence the Higgs couplings are proportional to the gauging of the symmetry (interactions  $\sim g, g'$ ) and the existence of a non-trivial vacuum (interactions  $\sim v$ ), which in turn depends on the presence of Higgs self-couplings

$$v = \sqrt{\frac{-\mu^2}{\lambda}}. \quad (2.67)$$

Re-introducing the dynamical Higgs field for the diagonal fermion interactions we obtain

$$\frac{y_f v}{\sqrt{2}} \bar{f} f \rightarrow m_f \bar{f} f \left( 1 + \frac{h}{v} \right), \quad (2.68)$$

which follows the same pattern and shows that the coupling strengths of the Higgs boson in the SM follow the fermions mass hierarchy.

### 2.3 Consistency checks of SM electroweak symmetry breaking

In unitary gauge we have effectively absorbed the Goldstone modes into the gauge fields. This shows most transparently that on top of two polarisations for massless gauge fields, we need to include longitudinal polarisations for massive gauge bosons, e.g.

$$\epsilon_L^\mu(p) = \frac{1}{m} \begin{pmatrix} p_z \\ 0 \\ 0 \\ E \end{pmatrix}, \text{ for } p^\mu = \begin{pmatrix} E \\ 0 \\ 0 \\ p_z \end{pmatrix}. \quad (2.69)$$

It is straightforward to see that indeed

$$\epsilon_L^\mu(p) k_\mu = 0 \quad \epsilon_L^2(p) = -1 \quad (2.70)$$

as we require for polarisation vectors. But also in the high-energy regime we essentially have

$$\epsilon_L^\mu(p) \simeq \frac{p^\mu}{m} \quad (E \gg m). \quad (2.71)$$

This can lead to a potentially dangerous growth of the amplitude leading to perturbatively unphysical consequences. In particular, by naive power counting, longitudinal  $W_L W_L \rightarrow W_L W_L$  scattering should behave at the amplitude level as (Fig. 3)

$$\mathcal{M} \sim \alpha^{(4)} E^4 + \alpha^{(2)} E^2 + \alpha^{(0)} E^0 + \dots \quad (2.72)$$

for energies well above the  $W$  mass. Perturbative unitarity constraints, on the other hand, can be formulated by analysing the amplitude for given angular momenta using partial waves [24, 25].

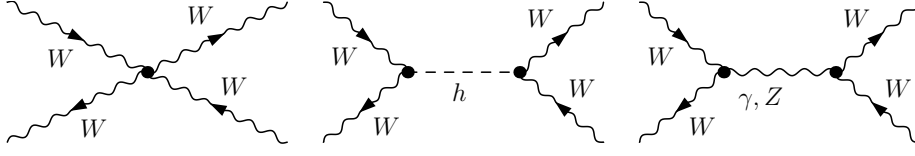


**Figure 3:** Feynman Diagrams contributing to  $WW$  scattering.  $t$  channel diagrams are not shown.

Typically the strongest constraint comes from the zeroth partial wave (unless it vanishes due to spin considerations), which can be formulated as

$$|\text{Re}(a_0)| < \frac{1}{2}, \quad a_0 = \frac{1}{16\pi s} \int_{-s}^0 |\mathcal{M}|. \quad (2.73)$$

where  $s = 4E^2$  (when  $E \gg m_W$ ). From this we can see that any energy growth of the amplitude as indicated in Eq. (2.72), will lead to unitarity violation at some scale.

As the Lagrangian is real, scattering processes should be unitary<sup>3</sup>, so a natural way of thinking of the breakdown of unitarity is that we have lost perturbative control. This means that subsequent corrections will become of equal size as the leading order (LO) approximation, ultimately restoring unitarity when we sum over sufficiently many terms in the perturbative series expansion. For particle physics as we know it, this would be rather catastrophic: We would need to assign a large uncertainty to our collider or even flavour predictions that arise from not knowing the higher-order terms.

In fact, the Higgs mass plays something like an order parameter of the electroweak series convergence and the energy growth is not as violent as we naively expect. This is due to our theory containing a large gauge symmetry. We can calculate the  $W_L W_L \rightarrow W_L W_L$  for general coupling strengths of the involved Feynman diagrams at LO. The cancellations of the terms  $\sim E^4, E^2$  then translate into two sum rules which highlight the interplay of the involved interactions for energies above all thresholds

$$\begin{aligned} \alpha^{(2)} : \quad & g_{WWWW} = g_{WW\gamma}^2 + g_{WWZ}^2, \\ \alpha^{(1)} : \quad & 4m_W^2 g_{WWWW} = 3m_Z^2 g_{WWZ}^2 + g_{WWh}^2. \end{aligned} \quad (2.74)$$

The  $WWWW$  vertex strength arises from the  $SU(2)_L$  kinetic term and therefore  $g_{WWWW} = g^2$ . The coupling strength of the  $WW\gamma$  vertex is simply  $e$ , while the  $WWZ$  interaction receives a modification due to the  $\cos \theta_w$  rotation  $g_{WWZ} = g \cos \theta_w$ . So

$$g_{WW\gamma}^2 + g_{WWZ}^2 = e^2 + g^2 \cos^2 \theta_w = g^2 (\sin^2 \theta_w + \cos^2 \theta_w) = g^2. \quad (2.75)$$

The cancellation of the  $\sim E^4$  growth is purely due to (linear) gauge invariance. We are left with an energy growth  $\sim E^2$ . Previously we have found that  $g_{WWh} = gm_W$  so

$$3m_Z^2 g_{WWZ}^2 + g_{WWh}^2 = 3m_Z^2 g^2 \cos^2 \theta_w + g^2 m_W^2 = 3m_W^2 g^2 + g^2 m_W^2 = 4g^2 m_W^2 \quad (2.76)$$

<sup>3</sup>One could bring up mathematical arguments against this, e.g. Stone's theorem does not necessarily translate to quantum field theories. However, given the success of the SM describing data, there is good ad-hoc reason to believe that our mathematical formulation of the QFT is reasonably good.

so also the  $\sim E^2$  growth is cancelled above the Higgs threshold due to non-linear gauge invariance. Similar sum rules can be formulated for all scattering processes [25, 26] (including fermions [27, 28]) and similar cancellations will appear. In fact we might be tempted to turn the argument around and ask: if we write down a general theory of massive gauge bosons and require a good high-energy behaviour, what are the consequences for the terms in the Lagrangian? It turns out that the collection of cancellations is equivalent to implementing a Higgs mechanism in some guise. It does not need to be the SM Higgs mechanism but needs to follow the concept of spontaneous symmetry breaking [6–8]. An important feature that we see from the  $\sim E^2$  sum rule is that if we push out the Higgs mass to large values, the intermediate  $\sim E^2$  will directly impact the convergence of the electroweak series. The discovery of a relatively light Higgs boson is, hence, not just a success for the SM alone but for perturbative QFTs in general.

To conclude our unitarity discussion, we quote the final result

$$a_0 = \frac{m_h^2}{8\pi v^2}. \quad (2.77)$$

So indeed the  $\alpha^{(0)}$  will be sensitive to the Higgs boson even above the Higgs threshold. Perturbative unitarity therefore gives an upper bound of  $m_h \lesssim 900$  GeV. It is not an accident that this is exactly the mass region that the LHC was constructed to look for the Higgs with high sensitivity. Indeed, before the Higgs discovery, the LHC was a no-lose experiment: We would either find the Higgs (very likely), or something spectacularly new that would enforce perturbative unitarity (less likely), or even see the very basis of quantum mechanics violated at high energies (least likely).

Although the Higgs boson has been observed at a mass range that is very consistent with this constraint, it is clear that if  $g_{WWH} \neq gm_W$  we face an immediate problem. Hence, if we stick to perturbative unitarity as a guiding concept any deviation of the Higgs coupling strengths from their SM expectation will imply new physics to compensate for this deviation.

We can look at a simple extension of the SM and its mechanism of electroweak symmetry breaking to see how this comes about. To this end, let us extend the SM Higgs sector with a singlet<sup>4</sup>

$$V = \mu_s^2 |\Phi_s|^2 + \lambda_s |\Phi_s|^4 + \mu_h^2 |\Phi_h|^2 + \lambda_h |\Phi_h|^4 + \eta_\chi |\Phi_s|^2 |\Phi_h|^2 \quad (2.78)$$

where  $s$  stands for our SM Higgs doublet and  $h$  is a hidden scalar. We can substitute

$$\Phi_i \rightarrow \frac{1}{\sqrt{2}}(v_i + h_i) \quad v_i^2 = \frac{1}{\lambda_j} \left( -\mu_i^2 - \frac{\eta_\chi v_j^2}{2} \right), \quad i, j = s, h. \quad (2.79)$$

As only the SM Higgs field couples to the SM gauge bosons  $v_s$  is fixed through  $m_W$ , while  $v_h$  is free. The mixing term then leads to a mixing of the Lagrangian eigenstates as both scalars obtain a vev

$$\eta_\chi \eta_\chi |\Phi_s|^2 |\Phi_h|^2 \supset \frac{\eta_\chi}{2} v_s v_h h_s h_h \implies \begin{pmatrix} h \\ H \end{pmatrix} = \begin{pmatrix} \cos \chi & -\sin \chi \\ \sin \chi & \cos \chi \end{pmatrix} \begin{pmatrix} h_s \\ h_v \end{pmatrix}. \quad (2.80)$$

<sup>4</sup>Also referred to as the Higgs portal as the Higgs is one of only three candidates that allows to portal to a hidden sector. The other two are  $U(1)_Y$  mixing, and mixing with a sterile right-handed neutrino.

As a consequence, the SM  $WW_h$  vertices are dressed with an angle  $\cos \chi$  and we have a new state with exactly the SM structure dressed with  $\sin \chi$ . For energies above  $m_h, m_H$  we therefore have

$$\alpha_{\text{Higgs}}^{(2)} : \quad g^2 m_W^2 \cos^2 \chi + g^2 m_W^2 \sin^2 \chi = g^2 m_W^2, \quad (2.81)$$

i.e. we recover exactly the SM Higgs contribution to  $W_L W_L$  scattering.

## 2.4 Electroweak precision observables

Of course, searches at the LHC and theoretical investigations are informed by earlier measurements. Possibly the most relevant in this context are the precision measurements during the LEP era. As detailed above, we can start stress-testing the electroweak Standard Model with four independent gauge sector measurements. Choosing as input parameters [29]

$$\begin{aligned} G_\mu &= 1.16638(1)^{-5} \text{ GeV}^{-2}, \\ \alpha &= 1/137.035999679(94), \\ m_Z &= 91.1876(21) \text{ GeV}, \end{aligned} \quad (2.82)$$

we can use the SM relations to predict the  $W$  boson mass via

$$m_W^2 = \frac{m_Z^2}{2} \left( 1 + \sqrt{1 - \frac{4\pi\alpha}{\sqrt{2}G_\mu m_Z^2}} \right) = (79.83 \text{ GeV})^2. \quad (2.83)$$

We can compare this to the measurement of the  $W$  mass [29]

$$m_W^{\text{obs}} = 80.379 \pm 0.012 \text{ GeV} \quad (2.84)$$

which is off by  $45 \sigma$ . “New physics!” I hear you scream, but this in fact only highlights the importance of electroweak corrections for precision observables.

A famous subset of electroweak precision corrections that has been used a lot in the theory community are the Peskin-Takeuchi parameters [30–32]. Under the assumption that new physics is heavy compared to the  $Z$  pole at which LEP gathered its data we can use an effective Lagrangian in the broken electroweak phase to study deformations of the gauge sector<sup>5</sup> by defining (we follow [33])

$$\mathcal{L}_{\text{eff}} = \mathcal{L}(\bar{e}_i) + \mathcal{L}_{\text{new}}. \quad (2.85)$$

The bar indicates SM quantities and relations and

$$\begin{aligned} \mathcal{L}_{\text{new}} = & -\frac{A}{4} \hat{F}_{\mu\nu} \hat{F}^{\mu\nu} - \frac{B}{2} \hat{W}_{\mu\nu}^+ \hat{W}^{-\mu\nu} - \frac{C}{4} \hat{Z}_{\mu\nu} \hat{Z}^{\mu\nu} + \frac{G}{2} \hat{F}_{\mu\nu} \hat{Z}^{\mu\nu} \\ & - w \hat{m}_W^2 \hat{W}_\mu^+ \hat{W}^{-\mu} - z \hat{m}_Z^2 \hat{Z}_\mu \hat{Z}^\mu, \end{aligned} \quad (2.86)$$

<sup>5</sup>This is another assumption of the Peskin-Takeuchi parameters: new physics should predominantly manifest itself in the gauge sector. This is true for broadly defined Higgs sector extensions.

where the hats indicate that the physical fields might differ from the Lagrangian fields<sup>6</sup>. As we would like to deal with canonically normalized fields we can redefine

$$\hat{A}_\mu = \left(1 - \frac{A}{2}\right) A_\mu + GZ_\mu, \quad (2.87)$$

$$\hat{W}_\mu^\pm = \left(1 - \frac{B}{2}\right) W_\mu^\pm, \quad (2.88)$$

$$\hat{Z}_\mu = \left(1 - \frac{C}{2}\right) Z_\mu, \quad (2.89)$$

and expand everything to linear order in the coefficients  $A, B, C, G$ . Then

$$\mathcal{L}_{\text{eff}} = \{\text{SM kinetic terms}\} + (1 + w - B)\bar{m}_W^2 W_\mu^+ W^{-\mu} + \frac{1}{2}(1 + z - C)\bar{m}_Z^2 Z_\mu Z^\mu \quad (2.90)$$

but the field redefinitions will also change the charged and neutral current interactions

$$\mathcal{L}_{\text{em}} = -\bar{e} \left(1 - \frac{A}{2}\right) \sum_i Q_i \bar{f}_i \gamma^\mu f_i A_\mu \quad (2.91)$$

$$\mathcal{L}_{\text{cc}} = -\frac{\bar{e}}{\sqrt{2}\bar{s}_\theta} \left(1 - \frac{B}{2}\right) \sum_i V_{ij} \bar{f}_i \gamma^\mu P_L f_j W_\mu^+ + \text{h.c.} \quad (2.92)$$

$$\mathcal{L}_{\text{nc}} = -\frac{\bar{e}}{\bar{s}_\theta \bar{c}_\theta} \left(1 - \frac{C}{2}\right) \sum_i \bar{f}_i \gamma^\mu (t_i^3 P_L - Q_i \bar{s}_\theta^2 + Q_i \bar{s}_\theta \bar{c}_\theta G) f_i Z_\mu, \quad (2.93)$$

where we have made explicit the  $SU(2)_L \times U(1)_Y$  covariant derivatives in the broken phase and traded  $\bar{g}, \bar{g}'$  for combinations of  $\bar{e}$  and  $\sin \bar{\theta}_w = \bar{s}_\theta$  and  $\cos \bar{\theta}_w = \bar{c}_\theta$  using SM relations (see above).

We can now give three of the theory parameters a meaning using measurements. Let us choose for convenience  $\bar{e}, \bar{m}_Z, \bar{s}_\theta$  (the latter through  $G_\mu$ ):

1.  $\bar{e}$  is conveniently measured in electron scattering at zero momentum transfer. This has the added advantage that all radiative corrections vanish in this limit where we measure the fine structure constant  $\alpha(Q^2 = 0)$

$$4\pi\alpha = \bar{e}^2(1 - A) = e^2 \quad (2.94)$$

where in the last part we use the SM relation between  $\alpha$  and  $e$  to *define*  $e$  (i.e. the relation to the measured input  $\alpha$  is understood implicitly). This gives us

$$\bar{e} = e \left(1 + \frac{A}{2}\right). \quad (2.95)$$

2. The  $Z$  mass is a straightforward pole measurement at  $s = m_Z^2$  giving

$$\bar{m}_Z^2 = m_Z^2(1 - z + C). \quad (2.96)$$

<sup>6</sup>There are many more operators that one could consider here, especially when we turn to the full dimension 6 deformation of the SM [34–36] (for a recent review see [37]).

3. Re-evaluating the Fermi constant in this new theory gives

$$\frac{G_\mu}{\sqrt{2}} = \frac{\bar{e}^2(1-B)}{8s_\theta^2\bar{m}_W^2(1+w-B)} = \frac{\bar{e}^2}{8s_\theta^2\bar{c}_\theta^2\bar{m}_Z^2}(1-w) \quad (2.97)$$

where we have used SM relations for the bar quantities  $\bar{m}_W = \bar{m}_Z\bar{c}_\theta$  and have expanded again to linear order in the deformations. Matching this again to the SM prediction

$$\frac{G_\mu}{\sqrt{2}} = \frac{e^2}{8s_\theta^2c_\theta^2m_Z^2} \quad (2.98)$$

allows us to define

$$\bar{s}_\theta^2 = s_\theta^2 \left( 1 + \frac{c_\theta^2}{c_\theta^2 - s_\theta^2} (A - C - w + Z) \right). \quad (2.99)$$

By construction we have

$$\mathcal{L}_Z \supset \frac{m_Z^2}{2} Z^\mu Z_\mu, \quad (2.100)$$

$$\mathcal{L}_{\text{em}} = -e \sum_i Q_i \bar{f}_i \gamma^\mu f_i A_\mu, \quad (2.101)$$

but the predicted  $W$  mass is now a complicated expression

$$m_W^2 = m_Z^2 c_\theta^2 \left( 1 - B + C - w - z - \frac{s_\theta^2}{c_\theta^2 - s_\theta^2} \{A - C - w + z\} \right) \quad (2.102)$$

and similarly for the neutral and charged current interactions. This shows that in general we will have  $m_W^2 \neq m_Z^2 c_\theta^2$  as the coefficients of Eq. (2.86) will appear when we consider quantum corrections in the SM. The physically relevant parameters are, however, not six as we are allowed to remove three of them through field redefinitions with no physically observable effect. So only three linear combinations enter physical observables, the Peskin-Takeuchi parameters

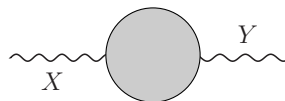
$$\alpha S = 4s_\theta^2 c_\theta^2 \left( A - C - \frac{c_\theta^2 - s_\theta^2}{c_\theta s_\theta} G \right), \quad (2.103)$$

$$\alpha T = w - z, \quad (2.104)$$

$$\alpha U = 4s_\theta^2 \left( A - \frac{B}{s_\theta^2} + \frac{c_\theta^2}{s_\theta^2} C - 2\frac{c_\theta}{s_\theta} G \right), \quad (2.105)$$

where we again understand the unbarred quantities in relation to measured input data, possibly using SM relations.

As we have only considered modifications of the field strengths and masses, all relevant information is contained in corrections to the gauge bosons' 2-point function. The Lorentz decomposition of these are



$$\Pi_{XY}^{\mu\nu}(p^2) = \Pi_{XY}(p^2)g^{\mu\nu} + B_{XY}(p^2)p^\mu p^\nu \quad (2.106)$$

(with  $X, Y = W, Z, A$ ). All field-strength and mass renormalization information is contained in  $\Pi_{XY}(p^2)$  [18] as well as its power series expansion around the physical masses, which allows us to write

$$\alpha S = \frac{4s_\theta^2 c_\theta^2}{m_Z^2} \left( \Pi_{ZZ}(m_Z^2) - \Pi_{ZZ}(0) - \Pi_{AA}(m_Z^2) - \frac{c_\theta^2 - s_\theta^2}{c_\theta s_\theta} (\Pi_{AZ}(m_Z^2) - \Pi_{AZ}(0)) \right), \quad (2.107)$$

$$\alpha T = \frac{\Pi_{WW}(0)}{m_W^2} - \frac{\Pi_{ZZ}(0)}{m_Z^2} - \frac{2s_\theta}{c_\theta} \frac{\Pi_{AZ}(0)}{m_Z^2}, \quad (2.108)$$

$$\alpha U = 4s_\theta^2 \left( \frac{\Pi_{WW}(m_W^2) - \Pi_{WW}(0)}{m_W^2} - c_\theta^2 \left( \frac{\Pi_{ZZ}(m_Z^2) - \Pi_{ZZ}(0)}{m_Z^2} \right) - 2s_\theta c_\theta \left( \frac{\Pi_{AZ}(m_Z^2) - \Pi_{AZ}(0)}{m_Z^2} \right) - s_\theta^2 \frac{\Pi_{AA}(m_Z^2)}{m_W^2} \right). \quad (2.109)$$

where we have already used  $\Pi_{AA}(0) = 0$  due to QED gauge-invariance.

Coming back to the problem of the  $W$ , we can look at the SM corrections. The  $T$  parameter measures the violation of the custodial isospin relation  $m_W = m_Z \cos \theta_W$  at a given charged-neutral current relation. Custodial isospin in the SM is broken by gauging hypercharge (i.e.  $\Phi^c$  and  $\Phi$  transform differently) as well as by fermionic mass differences within the weak doublets (the top mass enters non-logarithmically). This makes the top and Higgs contributions particularly relevant. The corrections to the  $W$  can be written as [38]

$$m_W^2 = \frac{\pi\alpha}{\sqrt{2}G_\mu s_\theta^2} [1 - \Delta r_{\text{SM}}] \quad (2.110)$$

where  $\Delta r_{\text{SM}}$  summarizes the SM contributions. The top contribution enters quadratically

$$\Delta r_{\text{SM}}^t = -\frac{G_\mu}{\sqrt{2}} \frac{3}{8\pi^2} \frac{c_\theta^2}{s_\theta^2} m_t^2 + \dots \quad (2.111)$$

where the ellipses refer to terms  $\sim \log m_t$ . The dependence on the Higgs mass is logarithmic

$$\Delta r_{\text{SM}}^h = \frac{\alpha}{\pi s_\theta^2} \frac{11}{48} \log \left( \frac{m_h^2}{m_Z^2} \right) + \dots \quad (2.112)$$

After the top quark discovery, the precision analysis of electroweak SM corrections were the most constraining ones regarding the Higgs mass, which was the only free parameter left at this point, see Fig. 4. Fits to the electroweak sector as performed by, e.g., the GFitter Collaboration are therefore strong tests of SM and BSM physics [39]. Not all electroweak corrections can be understood along the lines of  $S, T, U$  (or the extended set of [33, 40, 41]). As we have not made any specific reference to the fermion-gauge boson interactions apart from tracing effects in the gauge-boson two-point function, these can appear in addition to the ones we have discussed. As the gauge-boson corrections affect processes uniformly,  $S, T, U$  are often referred to as oblique corrections, whereas precision measurements of  $Z \rightarrow b\bar{b}$  are non-oblique in their nature.

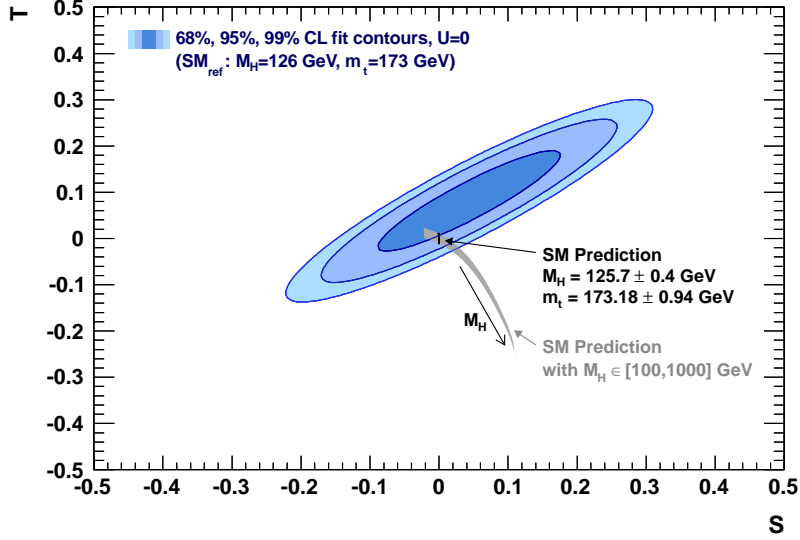


**Figure 4:** Allowed region of the  $S, T$  parameters after the Higgs discovery, assuming  $U = 0$ . Figure taken from [42].

We typically measure  $\Delta S, \Delta T, \Delta U$  against the SM best fit point, which makes calculations easier as Goldstone, ghost, or even subsets of SM contributions cancel. For instance if we go back to our singlet extension of the Higgs sector, we will find

$$\Delta S = \frac{1}{12\pi} \sin^2 \chi \log \left( \frac{m_H^2}{m_h^2} \right), \quad (2.113)$$

$$\Delta T = \frac{3}{16\pi \cos^2 \theta_w} \sin^2 \chi \log \left( \frac{m_H^2}{m_h^2} \right), \quad (2.114)$$

$$\Delta U = 0. \quad (2.115)$$

which provides a strong constraint on  $\sin^2 \chi$  as well as the mass of  $m_H$  if we assume  $m_h = 125$  GeV. The absence of a correction to  $U$  is not a coincidence but indicative of the fact that the power-counting of the effective field theory contributions to  $S, T$  arise at different operator dimensions.  $S, T$  arise at dimension 6

$$S \sim O_{WB} = (\Phi^\dagger t^a \Phi) W_{\mu\nu}^a B^{\mu\nu}, \quad (2.116)$$

$$T \sim O_H = (\Phi^\dagger D_\mu \Phi)^2. \quad (2.117)$$

## 2.5 Electroweak precision post Higgs discovery

Now that we have observed the Higgs boson, a natural progression of the previous discussion is the inclusion of the Higgs 2-point function, which also highlights a famous problem of the SM. Evaluating the shift of the Higgs pole in cut-off regularisation  $\sim \Lambda$  we find the famous Veltman condition [43]

$$\delta m_h^2 \sim (m_h^2 + 2m_W^2 + m_Z^2 - 4m_t^2) \frac{\Lambda^2}{v^2} \quad (2.118)$$

which gives rise to the Hierarchy Problem. It is not really a problem as it arises from using the same regularisation prescription for fermions as for scalars. There is no reason to do this; normally we would associate  $\Lambda$  with the cut-off of a more fundamental UV theory and e.g. in SUSY the gauge boson loops are regulated by gauginos while the top loop is mended by stops with different mass. Also quadratic divergencies are absent in dimensional regularisation.<sup>7</sup>

Following the discussion above, it is clear that whatever the mechanism that creates a weak scale value of the Higgs [44]

$$m_h = 125.09 \pm 0.21 \text{ (stat)} \pm 0.1 \text{ (syst)} \text{ GeV}, \quad (2.119)$$

we might only be able to observe it indirectly through its interaction deviations from the SM expectation. Or put in the words of electroweak renormalization: The Higgs mass is input data. Similar to the gauge bosons, the renormalization of the scalar Higgs boson includes a wave function part, which can be written as

$$\mathcal{L}_{\text{eff}} = \mathcal{L}_{\text{SM}} + \frac{1}{2} \delta Z_h \partial_\mu h \partial^\mu h. \quad (2.120)$$

Rescaling of the Higgs field shifts all Higgs couplings uniformly. So whatever might be responsible for the cancellations that guarantee a light Higgs boson, the associated dynamics might be visible in a universal modification of the Higgs couplings. This highlights future precision studies of the Higgs boson as a probe of TeV scale naturalness. The field strength modification is a dimension 6 operator

$$\delta Z_h \sim O_{\partial\Phi} = \partial_\mu (\Phi^\dagger \Phi) \partial^\mu (\Phi^\dagger \Phi) \quad (2.121)$$

which is good news! This means that there is no generic SM symmetry argument why effects should be suppressed above the TeV scale, i.e. they could be within the reach of future precision measurements. For instance, a precision study of associated Higgs production at a future lepton collider could constrain the cross section to 0.5% which can be translated to 10-25% tuning of Eq. (2.118) in concrete models [45].

### 3. Higgs production at hadron colliders

With the interaction rules of the previous section at hand, we are now in the position to study the dominant Higgs production and decay modes. For a more detailed review see [12].

#### 3.1 Higgs decay

The most relevant decay for a light Higgs boson is its decay into bottom quarks. Using standard techniques [46] that rely on the interaction terms we found earlier, one can obtain the partial decay widths

$$\Gamma(h \rightarrow f\bar{f}) = \frac{G_\mu m_f^2 N_c}{4\sqrt{2}\pi} m_h \sqrt{1 - \frac{4m_f^2}{m_h^2}}. \quad (3.1)$$

<sup>7</sup>What remains is a boundary setting problem in the deep UV. As the Higgs mass only runs moderately up to, say, the Planck scale  $M_{\text{Pl}} \sim 10^{19}$  GeV we have to ask ourselves what is the dynamics at the Planck scale that dynamically generates a dimensionless coupling  $m_h/M_{\text{Pl}} \sim 10^{-16}$  which should naively be of order 1? We are definitely missing something crucial here.

where  $N_c = 3$  (1) for quarks (leptons). QCD corrections are relevant and can be approximated by evaluating the quark mass at the Higgs pole, e.g.  $m_q = m_q(m_h^2)$  [47, 48]. We will content ourselves with leading order approximations to get a qualitative picture.

The decays to massive vector bosons is a little less straightforward as it involves including a vector boson decay  $h \rightarrow VV^* \rightarrow V + \text{fermions}$  ( $V = W, Z$ ). A careful analysis [49, 50] gives

$$\begin{aligned}\Gamma(h \rightarrow WW^*) &= \frac{3g^4 m_h}{512\pi^3} F\left(\frac{m_W}{m_h}\right) \\ \Gamma(h \rightarrow ZZ^*) &= \frac{g^4 m_h}{2048c_\theta^4 \pi^3} \left(7 - \frac{40}{3}s_W^2 + \frac{160}{9}s_W^4\right) F\left(\frac{m_Z}{m_h}\right),\end{aligned}\quad (3.2)$$

with

$$\begin{aligned}F(q) &= -|1 - q^2| \left( \frac{47}{2}q^2 - \frac{13}{2} + \frac{1}{q^2} \right) + 3(1 - 6q^2 + 4q^4)|\log q| \\ &\quad + \frac{3(1 - 8q^2 + 20q^4)}{\sqrt{4q^2 - 1}} \cos^{-1}\left(\frac{3q^2 - 1}{2q^3}\right).\end{aligned}\quad (3.3)$$

The decays to massless gauge bosons is particularly interesting as there is no tree-level coupling of the Higgs boson to photons or gluons. This means that although the diagrams are one-loop they have to be finite as there is no SM operator that can be renormalized. Explicit calculation of the  $h(k_1) \rightarrow g(k_2)g(k_3)$  amplitude gives

$$\mathcal{M} = \frac{\alpha_s y_t}{2\sqrt{2}\pi} \left( \varepsilon_2 \cdot \varepsilon_3 - \frac{2\varepsilon_2 \cdot k_1 \varepsilon_3 \cdot k_1}{m_t^2} \right) [m_t(m_h^2 - 4m_t^2)C_0(m_h^2, m_t^2) - 2m_t] \delta^{g_2 g_3} \quad (3.4)$$

where we use  $\varepsilon_i = \varepsilon(k_i)$  for the gluon polarisations and the  $\delta^{g_2 g_3}$  signalizes that the two gluons are in a colour-singlet configuration.  $C_0$  is a Passarino-Veltman [51] three-point scalar loop function. Its form is not too relevant at this point, but the whole expression behaves as  $\sim m_t^0 = 1$  for  $m_t \rightarrow \infty$ . So we see that, due to  $y_t \sim m_t/v$ , the top contributions will not decouple in this limit. Also we can see that the tensor structure of the interactions matches up with the dimension 6 effective operator

$$O_G = \Phi^\dagger \Phi G^{a\mu\nu} G_{\mu\nu}^a \supset \frac{\alpha_s}{12\pi} \frac{h}{v} G^{a\mu\nu} G_{\mu\nu}^a \quad (3.5)$$

where  $G_{\mu\nu}^a$  is the gluon field strength. This shows that indeed the  $h \rightarrow gg$  interaction formally arises from higher order SM corrections.

Using low-energy effective theory arguments [52–55] (for a contemporary treatment see [56]) this can be made more quantitative. Any amplitude that has an external Higgs leg coupling to a (virtual) fermion in the SM follows a pattern

$$\cdots \frac{i}{k-m} \frac{-im}{v} \frac{i}{k-p_h-m} \cdots \xrightarrow{p_h \rightarrow 0} \cdots \frac{-im}{v} \left[ \frac{1}{k-m} \right]^2 \cdots = \cdots \frac{im}{v} \frac{\partial}{\partial m} \left( \frac{1}{k-m} \right) \cdots \quad (3.6)$$

We can formalize this by writing a low-energy effective theorem (LET)

$$\lim_{p_h \rightarrow 0} \mathcal{M}(h+X) = \frac{m}{v} \frac{\partial}{\partial m} \mathcal{M}(X) \quad (3.7)$$

for unrenormalized quantities.  $\mathcal{M}(h+X)$  denotes the amplitude that arises by dressing  $\mathcal{M}(X)$  with a Higgs line in all possible ways. This allows us to reconstruct the effective Higgs-gluon interaction from the gluon kinetic term. Normalising

$$\mathcal{L}_{\text{QCD}} = -\frac{1}{4g_s^2} G_{\mu\nu}^{Ia} G^{Ia\mu\nu} \quad (G' = g_s G) \quad (3.8)$$

with the strong coupling  $g_s$  for convenience, we can apply the low-energy effective theorem

$$\mathcal{L}_{h+\text{QCD}} = -\frac{1}{4} \frac{h}{v} \left( m \frac{\partial}{\partial m} \frac{1}{g_s^2} \right) G_{\mu\nu}^{Ia} G^{Ia\mu\nu}. \quad (3.9)$$

The mass dependence of  $g_s$  follows from the QCD beta function

$$\beta(g_s) = \mu_R \frac{\partial g_s}{\partial \mu_R} \quad (3.10)$$

and specifically its dependence on the top quark

$$\beta^{m_t}(g_s) = \frac{\alpha_s}{6\pi} g_s \quad (3.11)$$

from which the effective operator Eq. (3.5) follows immediately. We can resum all  $h^n gg$  interactions in the compact form [56]

$$\mathcal{L}_{\text{LEFT}} = \frac{\alpha_s}{12\pi} G^{a\mu\nu} G_{\mu\nu}^a \log \left( 1 + \frac{h}{v} \right) \quad (3.12)$$

where the appearance of a log is directly related to the fact that  $m_t \sim y_t v$ .

As the top mass  $m_t \simeq 173$  GeV is not too far from the Higgs mass threshold effects are often non-negligible. The full  $m_t$  dependence for  $h \rightarrow gg$  was first worked out in the late 1970s giving [49, 57, 58]

$$\Gamma(h \rightarrow gg) = \frac{G_\mu \alpha_s^2 m_h^3}{64\sqrt{2}\pi^3} \left| \sum_q F_{1/2}(\tau_q) \right|^2, \quad (3.13)$$

where  $\tau_q \equiv 4m_q^2/m_h^2$  and the loop function is defined to be

$$F_{1/2}(\tau_q) \equiv -2\tau_q [1 + (1 - \tau_q)f(\tau_q)]. \quad (3.14)$$

It includes the fermion-Yukawa coupling  $\sim m_f$ , and a one-loop three-point function

$$f(\tau_q) = \begin{cases} [\sin^{-1} \sqrt{1/\tau_q}]^2, & \text{if } \tau_q \geq 1 \\ -\frac{1}{4} \left[ \log \frac{1 + \sqrt{1 - \tau_q}}{1 - \sqrt{1 - \tau_q}} - i\pi \right]^2, & \text{if } \tau_q < 1 \end{cases}. \quad (3.15)$$

Following similar strategies (this also applies to LET arguments), we can compute the partial decay width into photons

$$\Gamma(h \rightarrow \gamma\gamma) = \frac{\alpha^2 G_\mu}{128\sqrt{2}\pi^3} m_h^3 \left| \sum_f N_{c,f} Q_f^2 F_{1/2}(\tau_f) + F_1(\tau_W) \right|^2, \quad (3.16)$$

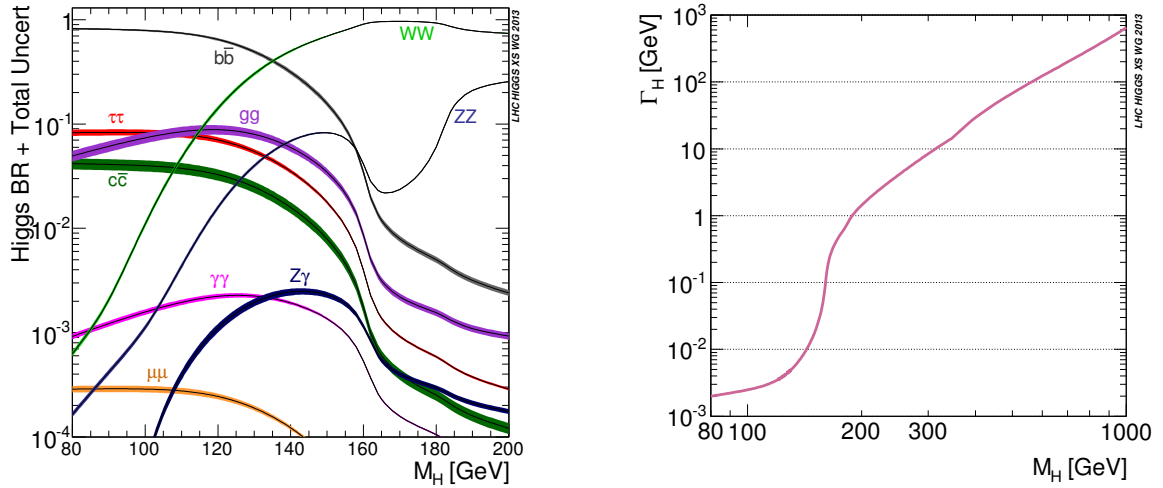


**Figure 5:** Higgs branching ratios and total Higgs decay width as reported by the CERN Higgs cross section working group including uncertainties. Figures taken from Ref. [59].

with

$$F_1(\tau) = 2 + 3\tau[1 + (2 - \tau)f(\tau)] \quad (3.17)$$

The limits  $\tau \rightarrow \infty$  give  $F_{1/2}(\infty) = -4/3$ ,  $F_1(\infty) = 7$  which shows a dedicated fermion-gauge boson interference of the decay  $h \rightarrow \gamma\gamma$ . In this sense, the decay of the Higgs into photons is a tell tale story of the mass generation in the fermion and gauge sector as well as their interplay.

The decays are summarized in Fig. 5. Although the Higgs boson is now firmly established at 125 GeV, the growth of the total decay with  $\sim m_h^3$  is interesting, in particular given its relation to the previous discussion of unitarity, electroweak precision constraints and convergence of the electroweak series. Naively, as  $m_t > m_W$  one could assume that for large Higgs masses the decay to top quarks would dominate, however the associated partial decay width grows  $\sim m_h$ . The large growth  $\sim m_h^3$  is entirely given by the Higgs decay to weak bosons. It is the Higgs boson's job to mend the growth of the amplitude of longitudinal vector bosons, i.e. it will couple more strongly, the larger the  $W$ 's energies will be. This is ultimately the reason why we see a dominant decay  $h \rightarrow WW/ZZ$  (the relative difference is entirely due to combinatorial factors from identical particle final states). In parallel this highlights the problem of the electroweak series convergence. For heavy Higgs boson masses the decay through  $W/Z$  bosons into multi-fermion final states will quickly outpace the prompt decays which are formally of lower-order perturbation theory [60]. It turns out that Nature is very kind to us and given the Higgs mass, we will be able to analyse the Higgs' phenomenology in a multitude of channels.

### 3.2 Higgs production

At hadron colliders, there are four main production modes for the Higgs boson: (i) gluon fusion  $pp \rightarrow h$ , (ii) weak boson fusion  $pp \rightarrow hjj$ , (iii) associated production  $pp \rightarrow hV$  ( $V = W, Z$ ) and (iv) top-associated Higgs production  $pp \rightarrow t\bar{t}h$ . General hadron collider cross sections follow

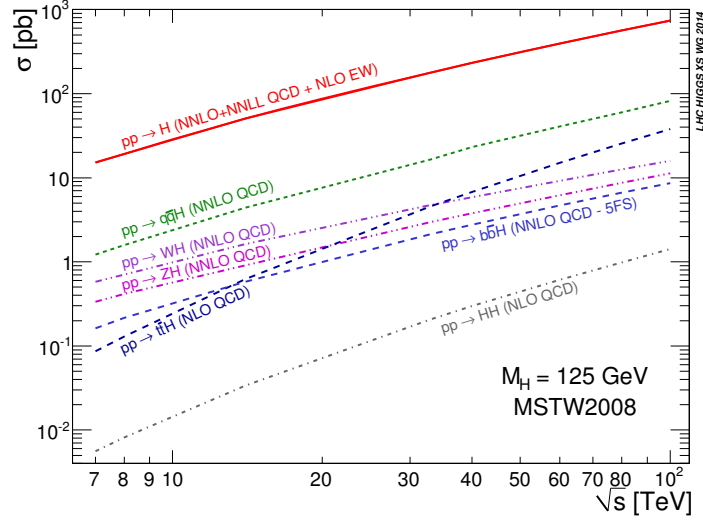


**Figure 6:** Production of the Higgs boson at hadron colliders with different center of mass energy from Ref. [66] including most known higher order corrections.

a factorisation which is qualitatively given by

$$d\sigma = [\text{flux factor}] \times \sum_{i,j} \int dx_1 \int dx_2 f_{i/p}(x_1 P_1, \mu_F^2) f_{j/p}(x_2 P_2, \tilde{\mu}_F^2) \times d\text{LIPS } \hat{\sigma}(ij \rightarrow f) \mathcal{F}(f \rightarrow j) \Theta(g(j)). \quad (3.18)$$

We extract from the protons with momenta  $P_{1,2}$ , partons (i.e. massless gluons and quarks)  $i$  and  $j$  with collinear momentum fractions  $x_{1,2}$ . The probability for this is given by the parton distribution functions (pdfs)  $f_{i,p}$  and  $f_{j,p}$ . The density of the initial states  $i, j$  is parametrized by the flux factor. The pdfs are intrinsically non-perturbative objects and need to be inferred by matching to (mostly deep inelastic scattering, DIS) data. They also depend on factorisation scales  $\mu_F$  and  $\tilde{\mu}_F$ , which makes an unphysical yet technically necessary distinction between non-perturbative and perturbative collinear energy scales. The extracted partons enter the hard scattering process to form a partonic final state  $f$  with partonic cross section  $\hat{\sigma}(ij \rightarrow f)$ . As we do not observe partons but hadrons we have to introduce a function that translates the partonic intermediate state into a jet-final state (e.g. a collimated splash of hadrons), which we call  $\mathcal{F}$ . Also, we typically have geometric acceptance cuts (e.g. particle detectors do not span a full solid angle) which are collected by the Heaviside function that acts on the jet-final states  $j$  with a possibly complicated function  $g$ .

The technical aspects of this prescription as well as its improvements could easily fill an own lecture course, and Frank Krauss' lectures at this school are an excellent resource (as is his recent book [61]). Here we limit ourselves to a qualitative motivation. The good news for the practitioners among you is that the technical aspects of these calculations have been automated to a large extent, and multi-purpose tools like MADEVENT [62], SHERPA [63], HERWIG [64] or WHIZZARD [65] will do the heavy-lifting (i.e. everything from Feynman Diagrams to the dLIPS phase space integration) for you.

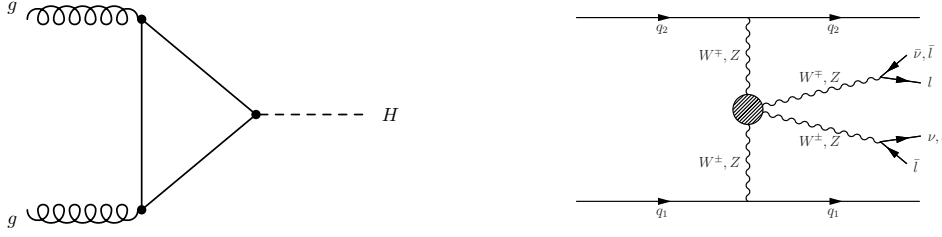


**Figure 7:** Left: Leading order diagram of gluon fusion  $gg \rightarrow h$ . The most dominant couplings arise from the top quark. Right: Weak boson fusion diagrams, the shaded region summarizes all electroweak contributions, including the Higgs, that are relevant for the unitarization of  $VV$  scattering. Diagrams with additional  $V$  emission off the quark legs are not shown.

### Gluon Fusion

As can be seen from Fig. 6, inclusive (i.e. no restrictions on the final state) gluon fusion (Fig. 7) is by far the most dominant production mechanism of the SM Higgs boson at proton-proton colliders. The partonic production cross section can be inferred from the decay width through unitarity considerations and is at leading order

$$\hat{\sigma}_{\text{LO}}(gg \rightarrow h) = \frac{\pi^2}{8m_h^2} \Gamma(h \rightarrow gg) \delta(\hat{s} - m_h^2) \quad (3.19)$$

where  $\hat{s} = (x_1 P_1 + x_2 P_2)^2$ . QCD corrections are quite large

$$K = \frac{\sigma_{\text{NLO}}}{\sigma_{\text{LO}}} \simeq 2 \quad (3.20)$$

as there is plenty of phase space available to emit extra jets, which is further enhanced by extra gluon emission “seeing” an effective colour charge of  $C_A = 3$ . The large  $K$ -factor does not signalize a breakdown of perturbation theory, but the LO colour singlet arrangement of the two gluons is somewhat unusual and a lot of colour combinatorics becomes available at NLO. As this cross section is particularly relevant for Higgs physics at the LHC it has been worked out to  $\text{N}^3\text{LO}$  precision in the  $m_t \rightarrow \infty$  limit [67], the current state-of-the-art.

### Weak Boson Fusion

The probably most non-QCD process that one can think of at hadron colliders is weak boson fusion [68–71], Fig. 7. It is another relevant process at the LHC as it accesses  $VV \rightarrow VV$  scattering and is therefore directly sensitive to the mechanism of unitarity conservation when new resonances compensate for deviations of the Higgs coupling from their SM expectation, in particular in gauge-philic scenarios [72].

WBF has a distinct signature, Fig. 8. To produce the Higgs we need to probe the incoming partons at relatively large momentum fractions, while their transverse momentum is roughly determined by the emitted vector boson [73]. This leads to very energetic jets at relatively low transverse

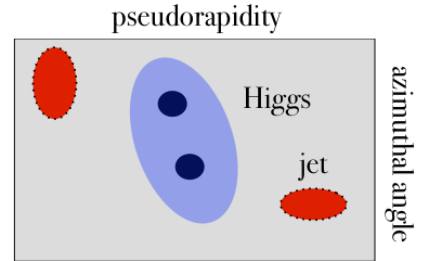


**Figure 8:** Typical weak boson fusion signature in the detector (pseudorapidity-azimuthal angle plane): Two energetic jets, largely separated in rapidity, with central Higgs decay products, free of central QCD activity.

momentum. As WBF at LO does only have trivial colour correlations, NLO QCD corrections do not involve a gluon exchange between the two quark lines (you cannot interfere a colour octet with a colour singlet configuration). The weak boson fusion topology is essentially two DIS diagrams glued together. This opens up the possibility to include the bulk of QCD corrections via smart choices of  $\mu_F, \tilde{\mu}_F$ . If the factorisation scales are chosen to be the  $t$ -channel momentum transfer of the respective quark line, the QCD corrections become  $\mathcal{O}(1\%)$  [74–78]. At this point we need to start worrying about electroweak corrections [79, 80].

Extra jet emission then follows a QED bremsstrahlung pattern, i.e. happens in the direction of the jets which are forward in the detector. The central part of the detector only contains the Higgs decay products. This means that this process through forward jets at large invariant mass with a central Higgs has great background suppression potential, in particular when we are interested in leptonic decay channels  $h \rightarrow VV^*$ . Most of the background and competing gluon fusion + 2 jet contributions which tend to be central can be effectively removed by vetoing QCD activity in the central part of the detector [81, 82]. This makes WBF also a formidable tool to look for invisibly-decaying Higgs bosons [83]. Such scenarios are particularly motivated when the hidden sector decays are mixed in Eq. (2.80).

### Associated Higgs Production

Associated Higgs production, typically  $pp \rightarrow hZ$  (Fig. 9), although not the most dominant Higgs production mode, has good phenomenological potential as the leptonically-decaying  $Z$  or  $W$  boson provides great way to trigger on the signature. In particular for the  $hZ$  production, backgrounds can be reduced to a large extent by requiring two light leptons of opposite charge and identical flavour,  $Z \rightarrow \mu^+\mu^-, e^+e^-$ . This also makes associated Higgs production another viable channel to look for invisible Higgs decays; associate production is under good perturbative control [84].

As the transverse momentum of the Higgs boson can be controlled through the recoil against the  $Z$  boson, we can probe very hard Higgs bosons in this channel. This has the advantage that dominant top backgrounds are largely suppressed for  $p_T(Z) \gtrsim 150$  GeV, but comes at the price of collimated Higgs decay products. In particular,  $h \rightarrow b\bar{b}$  with the largest branching fraction will then leave a “fat jet” signature as the bottoms are separated in the azimuthal-angle–pseudorapidity plane

$$\Delta R(b\bar{b}) = \sqrt{\Delta\phi^2 + \Delta\eta^2} \simeq \frac{m_h}{p_T(h)}. \quad (3.21)$$

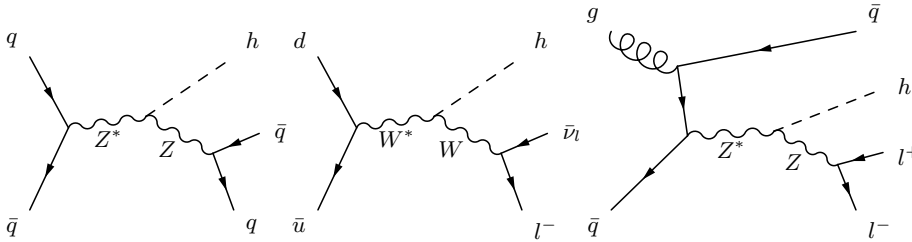


**Figure 9:** Leading order diagrams of associated Higgs production  $pp \rightarrow hV$ .

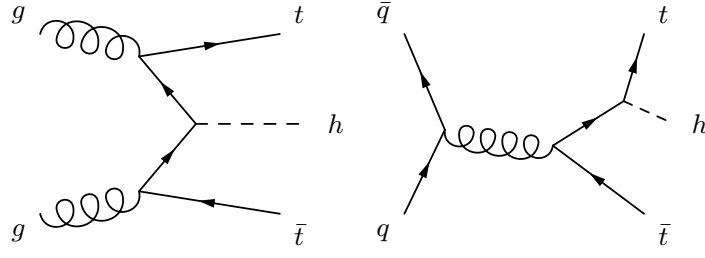


**Figure 10:** Leading order diagrams of top-associated Higgs production.

A strategy to isolate this signature from the contributing  $ZZ$  backgrounds was devised in [85], which led to the rapid development of the field of jet-substructure that has influenced collider physics tremendously over the past years (a nice summary is [86]). Jet-substructure techniques are now used in range of BSM searches not limited to Higgs physics.

### Top-associated Higgs Production

The production of a Higgs boson in association with two top quarks is the only process that has direct, tree-level sensitivity to the top Yukawa coupling. Hence, it is a key process for the Higgs phenomenology program.  $t\bar{t}h$  production is perturbatively under good control [87–94]. Originally proposed as the most sensitive mode to produce the Higgs at the LHC [95], more in-depth analyses toned down this expectation significantly [96]. Applications of jet substructure technology [97] revived the interest in this channel, and extended substructure techniques to the specifics of boosted tops in non-trivial ways (for a review see e.g. [98]).

Experimental efforts at the LHC currently heavily rely on the application of multivariate techniques [99, 100] that optimize the sensitivity along many different lines, many of which resting firmly in the experimental realm. It should be noted that this is also true for other rare Higgs production modes that are challenged by large backgrounds (e.g.  $V$ -associated production [101, 102]). This makes a re-analysis of experimental results by phenomenologists relatively difficult as the high-sensitivity analyses are necessarily non-transparent, but this will change as more data becomes available.

### 3.3 Higgs phenomenology: a tale of thresholds

In Fig. 11 we show the combination of Higgs-relevant data interpreted in a framework of coupling re-scalings

$$\kappa_X = \frac{g_{XXh}}{g_{XXh}^{\text{SM}}} \quad (3.22)$$

where  $X$  stands for allowed SM particles with couplings to the Higgs. As can be seen, although we are at a relatively early stage in the LHC program where sensitivity is driven by fairly inclusive measurements, there is compelling agreement with the SM hypothesis.

Total cross sections, branching ratios and  $N^{\text{th}}$ LO calculations, although undoubtedly crucial for Higgs phenomenology, are not always the most important factors of searches for deviations from the SM Higgs expectation. The development of boosted substructure approaches have highlighted the relevance of exclusive phase space regions for signal vs. background improvement whilst retaining a large enough sensitivity to the SM Higgs as well as deviations from the SM.

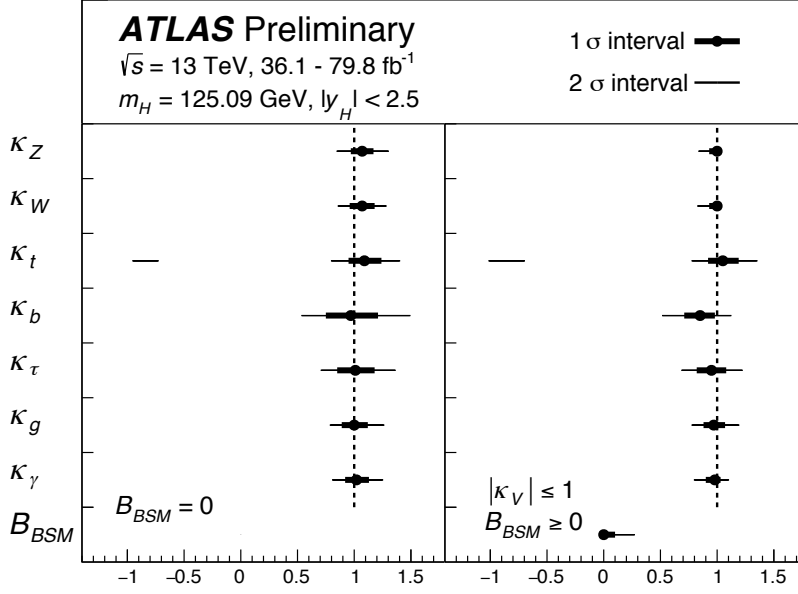


**Figure 11:** Fit of Higgs coupling deviations in the  $\kappa$  framework by ATLAS, taken from [103]. A flipped Yukawa sign for the top quark is excluded from the fit.

Thresholds play a particularly important role in this context. As one example of this, let us go back to  $Z$ -associated Higgs production where boosted selections become sensitive around  $p_T(Z) \gtrsim 150$  GeV.  $hZ$  production is dominated by quark-initial states, but at NNLO in QCD it will receive a finite gluon-induced component. The Feynman diagrams are pictured in Fig. 12. The top-threshold plays again a significant role as one can see in the distributions of Fig. 13. When we compare the  $q\bar{q} \rightarrow hZ$  production with the gluon fusion component we see that the gluon contribution follows a perturbative paradigm, i.e. it is only a small correction to the overall rate, but its contribution is entirely clustered above the  $2m_t$  threshold, which is a fairly exclusive region when comparing to the full  $m(hZ)$  spectrum. In parallel, the region selects transverse momenta of  $p_T(Z) \simeq p_T(h) \simeq m_t$ , which falls well into the coverage of boosted selection criteria. While in the SM the interplay of mass generation in the fermion sector and gauge boson sector leads to only a small correction, in models like the 2 Higgs doublet model [104, 105] where fermion masses are generated differently this correlation can be broken. In such scenarios the gluon fusion contribution carries significant information as is visible from Fig. 14 where parameter constraints are compared with and without  $gg \rightarrow hZ$  taken into account.

A second example where thresholds matter is the production of Higgs pairs. In our discussion of low-energy Higgs theorems we derived an expression for

$$\mathcal{L}_{\text{LEFT}} = \frac{\alpha_s}{12\pi} G^{a\mu\nu} G_{\mu\nu}^a \log\left(1 + \frac{h}{v}\right) \supset \frac{\alpha_s}{12\pi} G^{a\mu\nu} G_{\mu\nu}^a \left(\frac{h}{v} - \frac{h^2}{v^2}\right) \quad (3.23)$$

which highlights the destructive interference between the triangle diagrams and the box diagrams in Fig. 15, when taking  $m_t \rightarrow \infty$ . If we would like to access the trilinear Higgs self-coupling (which is related to quartic coupling  $\lambda$ )

$$\kappa_\lambda = \frac{g_{hhh}}{g_{hhh}^{\text{SM}}} = \frac{g_{hhh}}{6v\lambda} \quad (3.24)$$

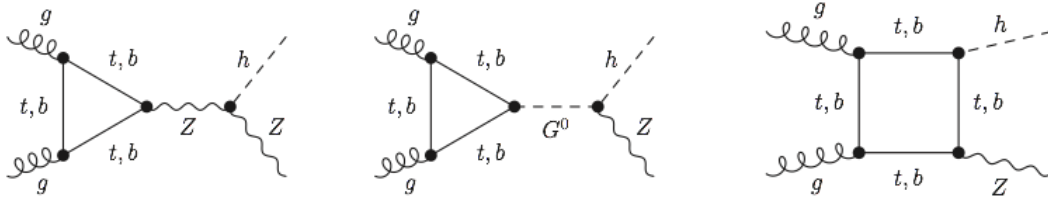


**Figure 12:** Feynman diagrams in general gauge contributing to  $gg \rightarrow hZ$ .

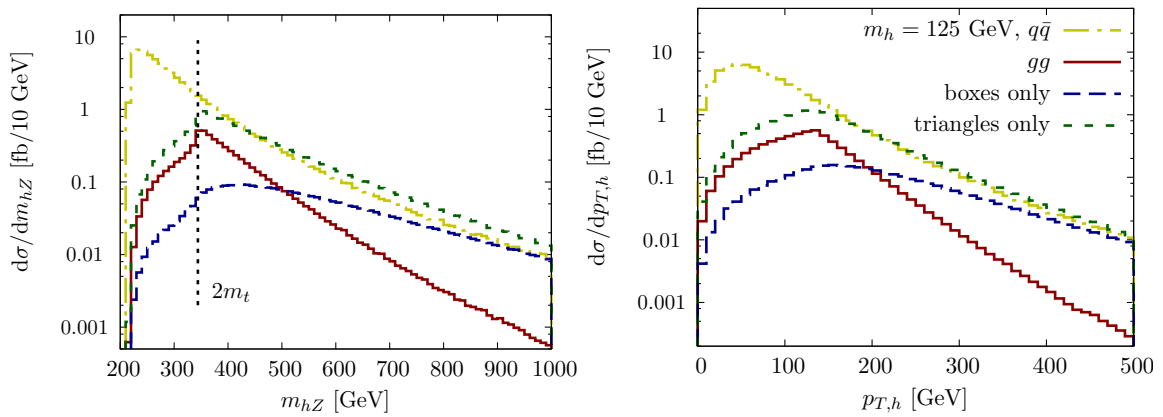


**Figure 13:** Invariant  $hZ$  mass and Higgs transverse momentum distributions of  $pp \rightarrow hZ$  highlighting the gluon fusion contribution and the interplay of box and triangle diagrams of Fig. 12. Taken from [104].

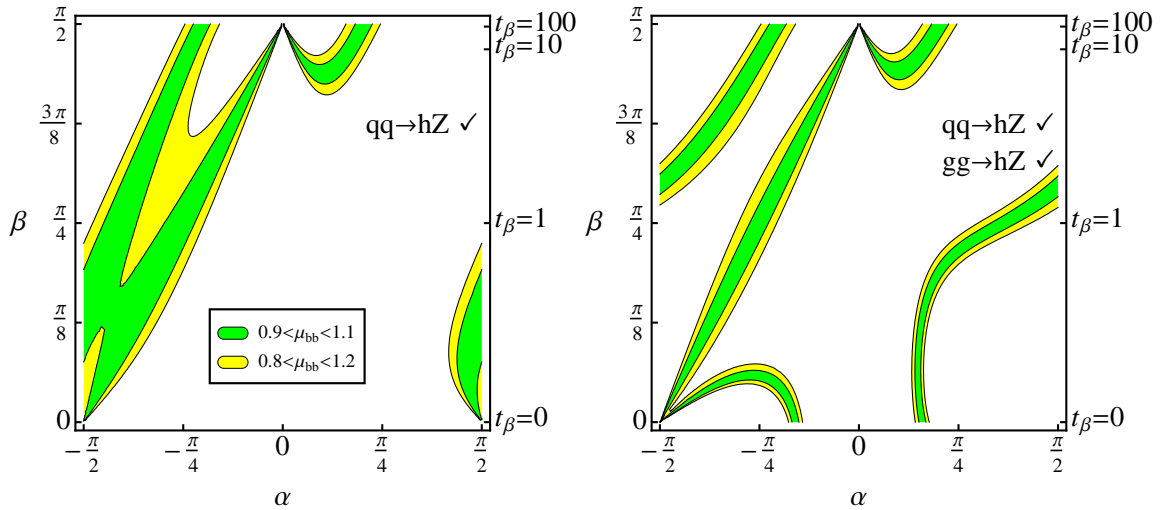


**Figure 14:** Boosted Higgs analysis in the context of a two Higgs doublet model using  $gg \rightarrow hZ$ . Taken from [104].

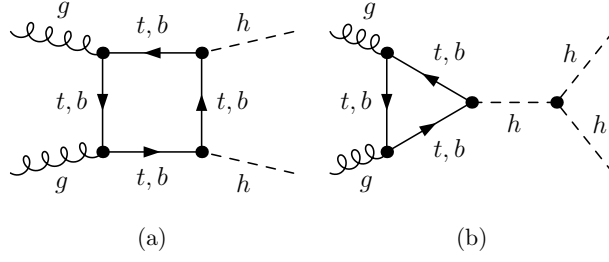


**Figure 15:** Feynman diagrams contributing to  $gg \rightarrow hh$  production.

this interference pattern is crucial. The dynamics of the triangle diagrams is already given by Eq. (3.15) by making the replacement  $m_h \rightarrow m(hh)$ , i.e. the virtual Higgs carries the invariant di-Higgs mass. The loop diagram reaches a maximum for  $m(hh) = 2m_t$  and as the continuum diagrams dominate we see a decreasing cross section when  $\kappa_\lambda > 1$  (until we enhance the triangles over the boxes for some large  $\kappa$ ). This is clearly visible in Fig. 16 where the prominent dip structure for  $p_T(h) \simeq 100$  GeV is directly related to the sensitivity around  $m(hh) \simeq 2m_t$ . The overall cross section of Higgs pair production at the LHC is relatively small (inclusive  $\sigma(gg \rightarrow hh) \simeq 32$  fb) which makes di-Higgs searches experimentally extremely difficult at the LHC in the motivated final states  $b\bar{b}\gamma\gamma$ ,  $b\bar{b}b\bar{b}$  and  $b\bar{b}\tau\tau$  [107–112]. Higgs pair production and its specific importance in BSM scenarios is a key motivation for a future hadron collider at high energy, possibly 100 TeV [113].

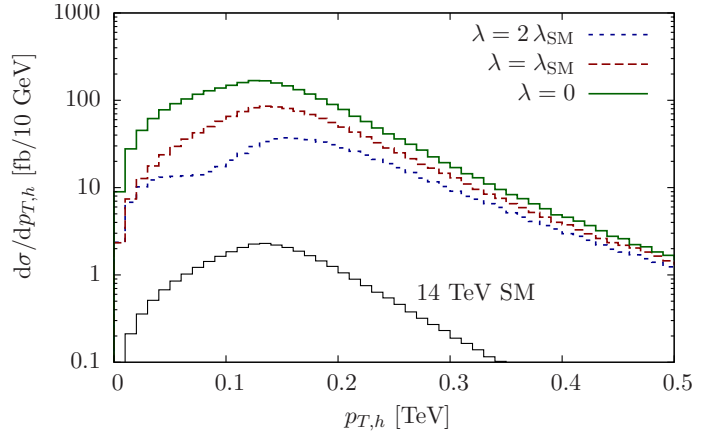


**Figure 16:** Transverse momentum distribution of the Higgs bosons in  $gg \rightarrow hh$  for 100 TeV. Taken from [106].

## 4. Higgs phenomenology post discovery

Higgs phenomenology has seen tremendous progress over the past years since the Higgs boson's discovery. Resonant extensions of the SM Higgs are widely discussed in the literature (see e.g. [12, 114]) and for these lectures we will limit ourselves to some aspects of effective field theory extensions of the SM.

### 4.1 Phenomenological aspects of Higgs sector EFT

The clear flaws of the SM have led to enormous model-building efforts over the past decades that aimed at mending at least some of the SM's shortcomings. Typically these come with concrete predictions, for instance a light supersymmetric top-partner to avoid the fine tuning indicated by Eq. (2.118). After the first few years of LHC running, most of these scenarios stand challenged;

no new physics seems to fall within of the current capabilities of the LHC. Taking this lack of evidence for new physics at face value, the theory community has turned increasingly to mostly model-independent methods to look for the presence of BSM physics through modifications of data correlations from their SM expectation. This does not mean that we will stop looking for Supersymmetry etc., it means that we are opening ourselves to the possibility that these concrete UV scenarios, as well-motivated as they might be, could be too limiting to be pursued as sole search strategies for new interactions.

The approach of choice, which has been successfully applied in the realm of flavour physics, is effective field theory. Concretely this means that we deform the SM Lagrangian with all a priori allowed  $d > 4$  higher dimensional operators, based on SM particle and symmetry content. Ignoring neutrino physics, these start at  $d = 6$ . We can expect a price for being phenomenologically holistic, and in fact there are 2499 operators that contribute at the  $d = 6$  level alone [36]. Many of these arise from four-fermion interactions highlighting the particular character of the SM flavour structure, and a lot of these operators can be further reduced by making symmetry-based assumptions. Nonetheless it is clear that the sheer number will imply a range of blind directions. Probably the most relevant to mention here in the light of our earlier discussion is the top Yukawa interaction that stands in competition with contact interactions (the  $m_t \rightarrow \infty$  limit).

This degeneracy can be broken by studying large momentum transfers, i.e. when we recoil the Higgs boson against a hard jet effectively introducing a new scale to the process that resolves the Compton wave length of the top quark. As can be seen in Fig. 17, even when the inclusive Higgs production cross section is consistent with the SM expectation through a cancellation between the interactions arising from

$$\mathcal{L}_{d6} = c_g \mathcal{O}_g + c_t \mathcal{O}_t = \frac{c_g \alpha_s}{12\pi v} h G^{a\mu\nu} G_{\mu\nu}^a + c_t h \bar{t} t, \quad (4.1)$$

the large  $p_T$  configurations resolve the degeneracy. Fig. 17 clearly shows that although there is good agreement for low momenta the missing absorptive parts of the amplitude (i.e. when we resolve  $\sqrt{\hat{s}} > 2m_t$ ) do lead to an increased cross section in the tail of the distribution when we have a contact interaction switched on. In a global fit to Higgs-sector relevant interactions (for recent results see [116–118]), this is key to lifting the  $c_g - c_t$  blind direction to constrain or observe the competing operators independently.

What Fig. 17 also suggests is that largest possible momentum transfers carry the most discriminating power. But this is not entirely true, which is visible from Fig. 18. In fact, given that

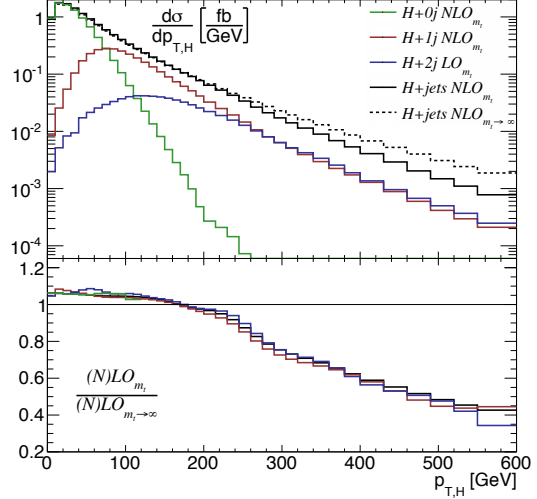


**Figure 17:** Higgs transverse momentum distribution for gluon fusion Higgs production with decay  $h \rightarrow W^+W^-$  obtained from jet-merged calculations in the finite  $m_t$  and  $m_t \rightarrow \infty$  limits. The  $m_t \rightarrow \infty$  calculation clearly overestimates the finite  $m_t$  expectation for large  $p_T$ . Figure taken from Ref. [115].

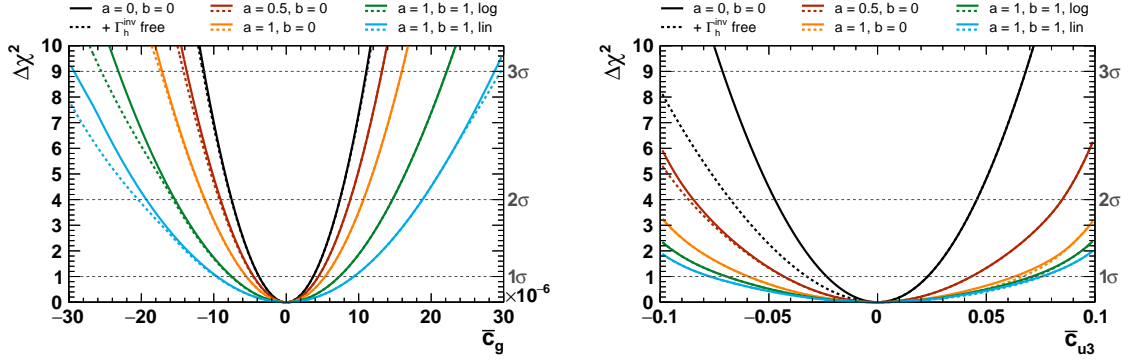


**Figure 18:** Expected sensitivity to contact interaction (left) and top-Yukawa modification (right) at  $3/ab$  in the normalisation of Ref. [119]. Figure taken from [120].

shapes of e.g.  $p_T(h)$  distributions are well-behaved functions for non-resonant extensions that do not show any BSM thresholds by construction, crucial shape deviations can already be sensitively assessed for comparably low transverse momenta. In Fig. 18 we compare the limits on  $c_g$  and  $c_t$  (in the normalisation of Ref. [119]) for modified uncertainties of the form

$$\delta(p_T(h)) = \delta_0[a + bf(p_T(h))] \quad (4.2)$$

with choices

$$f^{\log}(p_T(h)) = \log\left(1 + \frac{p_T(h)}{m_h}\right) \quad f^{\text{lin}}(p_T(h)) = \frac{p_T(h)}{m_h}. \quad (4.3)$$

This means that  $a$  determines the inclusive uncertainty, while  $b$  steers shape uncertainties for large  $p_T$ . In this case we compare a conservative linear scaling compared against a more realistic logarithmic behaviour expected from QCD [121]. The expected limits at  $3/ab$  for these choices are not that different which supports the statement that a global fit will always zero in on the sweet spot where the SM null hypothesis is under good theoretical and experimental control, and where the BSM contributions are just large enough to be statistically resolvable. Where exactly this phase space region sits highly depends on the assumptions that are made for the  $3/ab$  extrapolation, but surely it will not be the most exclusive phase space region that we can think of. Those are guaranteed to be under poor statistical and perturbative control.

There is a positive side effect of the more-inclusive-than-thought  $p_T$  selections: There is possibly large enough statistics to look for additional correlations in inclusive phase space regions through different observables other than  $p_T$  (or an alternative first-choice energy-dependent observable). Traditionally, this is done through imposing selection criteria to enhance the desired signal over the background (or SM expectation), but motivated by multivariate analysis techniques that have always been employed by experimentalists there is an increased focus on employing machine-learning techniques in the theory and phenomenology communities. The question that this addresses is the optimal information content of observables given expected BSM effects. This allows algorithms to adapt to particularly suited observable combinations and non-rectangular regions of phase space in terms of traditional collider observables such as  $p_T$ , invariant masses, rapidities or azimuthal angles. The result of distilling the information contained in such an ap-



spontaneously broken phase. For the purpose of these notes, where we would like to connect the Wilson coefficients to the “normal” running of SM couplings we therefore consider the earlier (and as it will turn out special) operator

$$\mathcal{L} = \mathcal{L}_{\text{SM}}^0 + \frac{c_G^0}{\Lambda^2} \underbrace{G_{\mu\nu 0}^a G_0^{a\mu\nu} \Phi_0^\dagger \Phi_0}_{=\mathcal{O}_{G,0}} \quad (4.4)$$

in the unbroken phase, where the “0” indicates that we are dealing with unrenormalized quantities. Multiplicative renormalization in dimensional regularisation  $d = 4 - 2\epsilon$  turns this Lagrangian into

$$\mathcal{L} = \mathcal{L}_{\text{SM}}(Z_G, Z_\Phi, \dots; G_R, \Phi_R, \dots) + Z_\Phi Z_G Z_c \mu^{-\epsilon} \frac{c_G}{\Lambda^2} G_{\mu\nu R}^a G_R^{a\mu\nu} \Phi_R^\dagger \Phi_R \quad (4.5)$$

with renormalization constants

$$X_0 = \sqrt{Z_X} X_R \quad (\text{with } Z_X = 1 + \delta Z_X) \quad (4.6)$$

where the index runs over all fields. For couplings we choose renormalization constants without the square root and drop the “R” index for convenience. The mass parameter  $\mu$  is introduced to keep the Wilson coefficient dimensionless in all  $d \neq 4$ .

To warm up, let us have a look at a very famous calculation, namely the  $\beta$  function of QCD, i.e. the scaling behaviour of the strong coupling constant  $g_s$ . We know that the SM is a renormalizable theory, so nothing bad should come our way here, and we will later apply the same techniques simply by interpreting the Wilson coefficient as the new coupling constant.

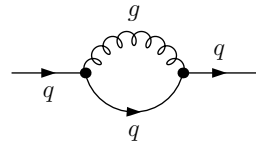
The relevant interaction that we would like to discuss arises for instance from the coupling of the gluon to a quark line

$$\mathcal{L}_{\text{SM}}^0 \supset -g_s^0 \bar{\psi}_0 \not{G}_0 \psi_0 = -g_s^0 \mathcal{O}_{\text{int},0}. \quad (4.7)$$

We have defined the local (unrenormalized) operator from the product of the involved quantum fields. We proceed by making the replacements

$$g_s^0 \bar{\psi}_0 \not{G}_0 \psi_0 = g_s^0 Z_\psi \sqrt{Z_G} \mathcal{O}_{\text{int},R} = \mu^\epsilon Z_{g_s} Z_\psi \sqrt{Z_G} g_s \mathcal{O}_{\text{int},R} = \mu^\epsilon Z_O g_s \mathcal{O}_{\text{int},R} \quad (4.8)$$

where we have again factorized out a mass scale  $\mu$  to make  $g_s$  dimensionless. To get the renormalization constant for strong coupling (and from that the RGE equation) we therefore need two ingredients: the gluon wave function renormalization constant and the quark renormalization constant (or equivalently the associated counterterms). We do not want to compute all these elements explicitly here, and just quote the results. Computing the one-loop 1PI correction to the  $\psi$  propagator we obtain



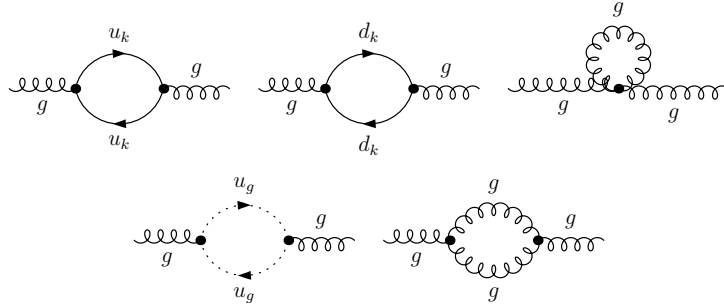
$$\delta Z_\psi = -\frac{g_s^2}{12\pi^2} \xi_G \Delta \quad (4.9)$$

where we only consider the divergent parts in dimensional regularisation, where infinities show up in the form of

$$\Delta = \left( \frac{4\pi\mu^2}{\mu_R^2} \right)^\epsilon \frac{\Gamma(1+\epsilon)}{\epsilon}. \quad (4.10)$$

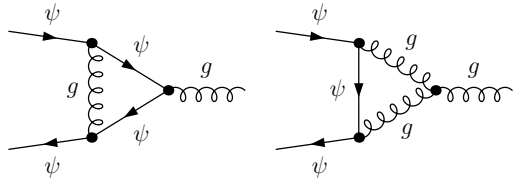
$\mu_R$  denotes the renormalization scale (here in the modified minimal subtraction scheme) and  $\xi_G$  is the gauge-fixing parameter of the gluon field.

In the next step we need to compute the field strength renormalization of the gluon field, which we obtain again from all 1PI corrections to the gluon propagator (summing over all quarks), leading to



$$\longrightarrow \delta Z_G = -\frac{g_s^2}{32\pi^2} (5 - 3\xi_G) \Delta. \quad (4.11)$$

With these two ingredients we can now go back and compute the amputated, connected 3-point function that arises from our operator. We can compute the Feynman Diagrams to obtain an expression



$$\longrightarrow \mathcal{M} = \mu^\epsilon Z_O g_s \langle \mathcal{O}_{\text{int},R} \rangle. \quad (4.12)$$

where  $\langle \dots \rangle$  stands for the contracted polarisation etc. With this and Eq. (4.8) we can identify

$$\delta Z_{g_s} = \delta Z_O - \delta Z_\psi - \frac{1}{2} \delta Z_G \quad (4.13)$$

with counterterm

$$\delta Z_O = -\frac{g_s^2}{48\pi} \Delta (27 + 25\xi_G) \quad (4.14)$$

and obtain

$$\delta Z_{g_s} = -\frac{7g_s^2}{8\pi^2} \Delta \quad (4.15)$$

which is independent of the gauge-fixing parameter as we would expect from our discussion in Sec. 2.1. From this, using the invariance of the bare coupling, we can obtain a RGE

$$\beta(g_s) = \lim_{\epsilon \rightarrow 0} \mu_R \frac{\partial g_s(g_s^0, \mu^\epsilon, \mu, \mu_R)}{\partial \mu_R} = -g_s \mu_R \frac{\partial \delta Z_{g_s}}{\partial \mu_R} = -\frac{7g_s^3}{16\pi^2} = -\beta_0 \frac{g_s^3}{16\pi^2}, \quad (4.16)$$

which is exactly the leading order beta function of QCD.<sup>8</sup> We can apply the same technique to the fixed order renormalization of our Wilson coefficient in Eq. (4.5). We already have the

<sup>8</sup>Often you see this result expressed in terms of Casimir of the adjoint representation  $C_A$  and the Dynkin index  $T_R$ ,  $\beta_0 = (11/3)C_A - (4/3)T_R$ .

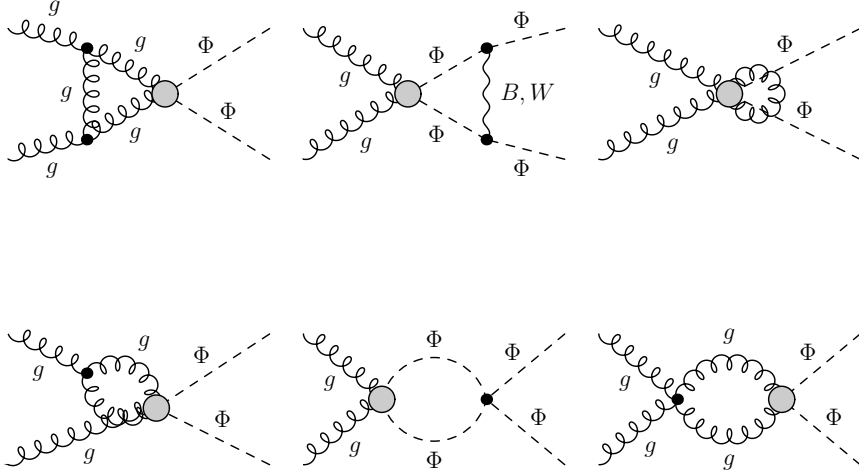


**Figure 20:** Representative one-loop corrections to the operator  $\mathcal{O}_G$  discussed in the text. The operator insertion is highlighted by the shaded region while the black vertices refer to SM couplings.

gluon wavefunction renormalization constant. So the next relevant quantity is Higgs wave function renormalization, which follows from all one-loop 1PI diagrams contributing to the Higgs 2-point function. The result for this is (we neglect Yukawa interactions in the following)

$$\delta Z_\Phi = \frac{1}{64\pi^2} (3g'^2 + 9g^2 + g'^2\xi_B - 3g^2\xi_W) \Delta \quad (4.17)$$

where the  $\xi_{B,W}$  refer to the different gauge-fixing parameters of the hypercharge and weak interactions.

With this we have enough to compute  $Z_c$  at one-loop order from the operator's amputated, connected Green's function, Fig. 20. Neglecting dimension 8 insertions, Fig. 21, (which is necessary for the general technical renormalization of dimension 6 interactions as explained above) the divergent parts of all one-loop corrections to the connected, amputated Green's function are

$$\begin{aligned} \mathcal{M} &= \mu^{-\varepsilon} c_G Z_{\mathcal{O}_G} \langle \mathcal{O}_{G,R} \rangle \\ &= \mu^{-\varepsilon} c_G \left[ 1 - \frac{\Delta}{64\pi^2} (g'^2\xi_B + 3[6g_s^2 - 8\lambda + 2g_s^2\xi_G + g^2\xi_W]) \right] \langle \mathcal{O}_{G,R} \rangle \end{aligned} \quad (4.18)$$

Therefore, modulo finite terms, we can write

$$\begin{aligned} \delta Z_c &= \delta Z_{\mathcal{O}_G} - \delta Z_\Phi - \delta Z_G \\ &= -\frac{\Delta}{64\pi^2} (3g'^2 + 9g^2 + 13g_s^2 - 24\lambda) . \end{aligned}$$

which gives rise to a RGE equation (see also [123, 127])

$$\lim_{\varepsilon \rightarrow 0} \mu_R \frac{\partial c_G}{\partial \mu_R} = \frac{1}{16\pi^2} \left( -\frac{3}{2}g'^2 - \frac{9}{2}g^2 + 12\lambda - 14g_s^2 \right) c_G . \quad (4.19)$$

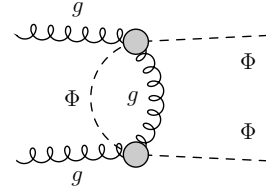


**Figure 21:** Representative double  $d = 6$  insertion leading to a  $d = 8$  interaction, which are not considered here.

The factor of  $-2\beta_0 g_s^2$  dominates the RGE flow. It can be absorbed by additionally normalising the operator with an additional factor  $g_s^2$ , which QCD RGE-improves fixed order calculations in Monte Carlo calculations. This is not a coincidence but related to the fact that the operator

$$\frac{\beta(g_s)}{g_s} G_{\mu\nu}^a G^{a\mu\nu} \quad (4.20)$$

is not renormalized to all orders in perturbation theory. If we change  $c_G = g_s^2 c_G^{g_s}$  we need to modify Eq. (4.19) with an additional factor  $-2\delta Z_{g_s} = 14g_s^2$  on the right hand side, which cancels the strong coupling constants in the modified RGE equation for  $c_G^{g_s}$ .

## 5. Summary and Outlook

With the Higgs boson firmly established at the LHC and the first data runs completed, the Higgs boson remains at the heart of the LHC phenomenology program some 6 years after its discovery. The current  $\mathcal{O}(10\%)$  coupling measurements are consistent with the electroweak precision studies performed at LEP, but the LHC is starting to push beyond these precision measurements in many areas of phenomenology. The Higgs through its special relation to the TeV scale, its particular quantum numbers and as the only potentially fundamental scalar we have seen in nature leaves us with a plethora of open questions. The LHC will clarify these when more data will become available.

The SM does not address a plethora of apparent BSM effects. These range from missing dark matter over insufficient CP violation to neutrino physics. The Hierarchy Problem remains puzzling, in particular in the light of the currently negative outcome of searches for exotics and the need for a new fundamental scale of physics. Over the next years, as we will gain a more fine-grained picture of the Higgs boson and its interactions in more general formulations of the weak scale addressing these questions, at least partially, will become possible. In parallel, LHC “blind spots” revealed by a more model-independent look at data-correlations that we discussed will provide a new strategy to look for BSM interactions beyond the old paradigms, also informing future collider cases such as an  $e^+e^-$  or a 100 TeV  $pp$  machine.

## Acknowledgements

Contributing to TASI as a lecturer is a privilege. I would like to thank the organizers of TASI 2018, Tilman Plehn and Tracy Slatyer, for giving me the opportunity to talk about a subject that is close to my heart. I would like to thank Tom Degrand for the great local organization. My special thanks go to the TASI 2018 students for indulging me and for creating a great and lively atmosphere.

I acknowledge support by the UK Science and Technology Facilities Council (STFC) under grant ST/P000746/1.

## References

- [1] F. Englert and R. Brout, “Broken Symmetry and the Mass of Gauge Vector Mesons,” *Phys. Rev. Lett.* **13** (1964) 321–323. [157(1964)].

- [2] P. W. Higgs, “Broken Symmetries and the Masses of Gauge Bosons,” *Phys. Rev. Lett.* **13** (1964) 508–509. [160(1964)].
- [3] P. W. Higgs, “Broken symmetries, massless particles and gauge fields,” *Phys. Lett.* **12** (1964) 132–133.
- [4] E. Fermi, “An attempt of a theory of beta radiation. 1.,” *Z. Phys.* **88** (1934) 161–177.
- [5] G. ’t Hooft, “Under the spell of the gauge principle,” *Adv. Ser. Math. Phys.* **19** (1994) 1–683.
- [6] C. H. Llewellyn Smith, “High-Energy Behavior and Gauge Symmetry,” *Phys. Lett.* **46B** (1973) 233–236.
- [7] J. M. Cornwall, D. N. Levin, and G. Tiktopoulos, “Uniqueness of spontaneously broken gauge theories,” *Phys. Rev. Lett.* **30** (1973) 1268–1270. [Erratum: *Phys. Rev. Lett.* 31,572(1973)].
- [8] J. M. Cornwall, D. N. Levin, and G. Tiktopoulos, “Derivation of Gauge Invariance from High-Energy Unitarity Bounds on the s Matrix,” *Phys. Rev.* **D10** (1974) 1145. [Erratum: *Phys. Rev.* D11,972(1975)].
- [9] P. W. Anderson, “Plasmons, Gauge Invariance, and Mass,” *Phys. Rev.* **130** (1963) 439–442. [153(1963)].
- [10] S. R. Coleman and J. Mandula, “All Possible Symmetries of the S Matrix,” *Phys. Rev.* **159** (1967) 1251–1256.
- [11] S. Dawson, “Electroweak Symmetry Breaking and Effective Field Theory,” in *Proceedings, Theoretical Advanced Study Institute in Elementary Particle Physics: Anticipating the Next Discoveries in Particle Physics (TASI 2016): Boulder, CO, USA, June 6–July 1, 2016*, pp. 1–63. 2017. [arXiv:1712.07232](https://arxiv.org/abs/1712.07232) [hep-ph].
- [12] S. Dawson, C. Englert, and T. Plehn, “Higgs Physics: It ain’t over till it’s over,” [arXiv:1808.01324](https://arxiv.org/abs/1808.01324) [hep-ph].
- [13] K. Fujikawa, B. W. Lee, and A. I. Sanda, “Generalized Renormalizable Gauge Formulation of Spontaneously Broken Gauge Theories,” *Phys. Rev.* **D6** (1972) 2923–2943.
- [14] C. Becchi, A. Rouet, and R. Stora, “The Abelian Higgs-Kibble Model. Unitarity of the S Operator,” *Phys. Lett.* **52B** (1974) 344–346.
- [15] C. Becchi, A. Rouet, and R. Stora, “Renormalization of the Abelian Higgs-Kibble Model,” *Commun. Math. Phys.* **42** (1975) 127–162.
- [16] C. Becchi, A. Rouet, and R. Stora, “Renormalization of Gauge Theories,” *Annals Phys.* **98** (1976) 287–321.
- [17] I. V. Tyutin, “Gauge Invariance in Field Theory and Statistical Physics in Operator Formalism,” [arXiv:0812.0580](https://arxiv.org/abs/0812.0580) [hep-th].
- [18] A. Denner, “Techniques for calculation of electroweak radiative corrections at the one loop level and results for W physics at LEP-200,” *Fortsch. Phys.* **41** (1993) 307–420, [arXiv:0709.1075](https://arxiv.org/abs/0709.1075) [hep-ph].
- [19] S. Weinberg, “A Model of Leptons,” *Phys. Rev. Lett.* **19** (1967) 1264–1266.
- [20] S. L. Glashow, “Partial Symmetries of Weak Interactions,” *Nucl. Phys.* **22** (1961) 579–588.
- [21] J. Goldstone, A. Salam, and S. Weinberg, “Broken Symmetries,” *Phys. Rev.* **127** (1962) 965–970.
- [22] A. Salam and J. C. Ward, “Electromagnetic and weak interactions,” *Phys. Lett.* **13** (1964) 168–171.

- [23] M. Bohm, A. Denner, and H. Joos, *Gauge theories of the strong and electroweak interaction*. 2001.
- [24] M. Jacob and G. C. Wick, “On the general theory of collisions for particles with spin,” *Annals Phys.* **7** (1959) 404–428. [Annals Phys.281,774(2000)].
- [25] B. W. Lee, C. Quigg, and H. B. Thacker, “Weak Interactions at Very High-Energies: The Role of the Higgs Boson Mass,” *Phys. Rev.* **D16** (1977) 1519.
- [26] B. W. Lee, C. Quigg, and H. B. Thacker, “The Strength of Weak Interactions at Very High-Energies and the Higgs Boson Mass,” *Phys. Rev. Lett.* **38** (1977) 883–885.
- [27] M. S. Chanowitz, M. A. Furman, and I. Hinchliffe, “Weak Interactions of Ultraheavy Fermions,” *Phys. Lett.* **78B** (1978) 285.
- [28] M. S. Chanowitz, M. A. Furman, and I. Hinchliffe, “Weak Interactions of Ultraheavy Fermions. 2.,” *Nucl. Phys.* **B153** (1979) 402–430.
- [29] **Particle Data Group** Collaboration, M. Tanabashi *et al.*, “Review of Particle Physics,” *Phys. Rev.* **D98** no.~3, (2018) 030001.
- [30] M. E. Peskin and T. Takeuchi, “A New constraint on a strongly interacting Higgs sector,” *Phys. Rev. Lett.* **65** (1990) 964–967.
- [31] M. E. Peskin and T. Takeuchi, “Estimation of oblique electroweak corrections,” *Phys. Rev.* **D46** (1992) 381–409.
- [32] G. Altarelli and R. Barbieri, “Vacuum polarization effects of new physics on electroweak processes,” *Phys. Lett.* **B253** (1991) 161–167.
- [33] C. P. Burgess, S. Godfrey, H. Konig, D. London, and I. Maksymyk, “A Global fit to extended oblique parameters,” *Phys. Lett.* **B326** (1994) 276–281, [arXiv:hep-ph/9307337](#) [hep-ph].
- [34] W. Buchmuller and D. Wyler, “Effective Lagrangian Analysis of New Interactions and Flavor Conservation,” *Nucl. Phys.* **B268** (1986) 621–653.
- [35] K. Hagiwara, R. D. Peccei, D. Zeppenfeld, and K. Hikasa, “Probing the Weak Boson Sector in  $e^+e^- \rightarrow W^+W^-$ ,” *Nucl. Phys.* **B282** (1987) 253–307.
- [36] B. Grzadkowski, M. Iskrzynski, M. Misiak, and J. Rosiek, “Dimension-Six Terms in the Standard Model Lagrangian,” *JHEP* **10** (2010) 085, [arXiv:1008.4884](#) [hep-ph].
- [37] I. Brivio and M. Trott, “The Standard Model as an Effective Field Theory,” [arXiv:1706.08945](#) [hep-ph].
- [38] W. J. Marciano and A. Sirlin, “Testing the Standard Model by Precise Determinations of  $W^+$ - and  $Z$  Masses,” *Phys. Rev.* **D29** (1984) 945. [Erratum: Phys. Rev.D31,213(1985)].
- [39] **Gfitter Group** Collaboration, M. Baak, J. CÅžth, J. Haller, A. Hoecker, R. Kogler, K. MÅnig, M. Schott, and J. Stelzer, “The global electroweak fit at NNLO and prospects for the LHC and ILC,” *Eur. Phys. J.* **C74** (2014) 3046, [arXiv:1407.3792](#) [hep-ph].
- [40] I. Maksymyk, C. P. Burgess, and D. London, “Beyond S, T and U,” *Phys. Rev.* **D50** (1994) 529–535, [arXiv:hep-ph/9306267](#) [hep-ph].
- [41] R. Barbieri, A. Pomarol, R. Rattazzi, and A. Strumia, “Electroweak symmetry breaking after LEP-1 and LEP-2,” *Nucl. Phys.* **B703** (2004) 127–146, [arXiv:hep-ph/0405040](#) [hep-ph].
- [42] M. Baak, M. Goebel, J. Haller, A. Hoecker, D. Kennedy, R. Kogler, K. Moenig, M. Schott, and J. Stelzer, “The Electroweak Fit of the Standard Model after the Discovery of a New Boson at the LHC,” *Eur. Phys. J.* **C72** (2012) 2205, [arXiv:1209.2716](#) [hep-ph].

- [43] M. J. G. Veltman, “The Infrared - Ultraviolet Connection,” *Acta Phys. Polon.* **B12** (1981) 437.
- [44] ATLAS, CMS Collaboration, G. Aad *et al.*, “Combined Measurement of the Higgs Boson Mass in  $pp$  Collisions at  $\sqrt{s} = 7$  and 8 TeV with the ATLAS and CMS Experiments,” *Phys. Rev. Lett.* **114** (2015) 191803, [arXiv:1503.07589 \[hep-ex\]](#).
- [45] N. Craig, C. Englert, and M. McCullough, “New Probe of Naturalness,” *Phys. Rev. Lett.* **111** no.~12, (2013) 121803, [arXiv:1305.5251 \[hep-ph\]](#).
- [46] A. Djouadi, “The Anatomy of electro-weak symmetry breaking. I: The Higgs boson in the standard model,” *Phys. Rept.* **457** (2008) 1–216, [arXiv:hep-ph/0503172 \[hep-ph\]](#).
- [47] A. Dabelstein and W. Hollik, “Electroweak corrections to the fermionic decay width of the standard Higgs boson,” *Z. Phys.* **C53** (1992) 507–516.
- [48] B. A. Kniehl, “Higgs phenomenology at one loop in the standard model,” *Phys. Rept.* **240** (1994) 211–300.
- [49] T. G. Rizzo, “Decays of Heavy Higgs Bosons,” *Phys. Rev.* **D22** (1980) 722.
- [50] W.-Y. Keung and W. J. Marciano, “Higgs Scalar Decays:  $h \rightarrow WX$ ,” *Phys. Rev.* **D30** (1984) 248.
- [51] G. Passarino and M. J. G. Veltman, “One Loop Corrections for  $e^+ e^-$  Annihilation Into  $\mu^+ \mu^-$  in the Weinberg Model,” *Nucl. Phys.* **B160** (1979) 151–207.
- [52] J. R. Ellis, M. K. Gaillard, and D. V. Nanopoulos, “A Phenomenological Profile of the Higgs Boson,” *Nucl. Phys.* **B106** (1976) 292.
- [53] M. A. Shifman, A. I. Vainshtein, M. B. Voloshin, and V. I. Zakharov, “Low-Energy Theorems for Higgs Boson Couplings to Photons,” *Sov. J. Nucl. Phys.* **30** (1979) 711–716. [*Yad. Fiz.*30,1368(1979)].
- [54] A. I. Vainshtein, V. I. Zakharov, and M. A. Shifman, “Higgs Particles,” *Sov. Phys. Usp.* **23** (1980) 429–449. [*Usp. Fiz. Nauk*131,537(1980)].
- [55] M. B. Voloshin, “Once Again About the Role of Gluonic Mechanism in Interaction of Light Higgs Boson with Hadrons,” *Sov. J. Nucl. Phys.* **44** (1986) 478. [*Yad. Fiz.*44,738(1986)].
- [56] B. A. Kniehl and M. Spira, “Low-energy theorems in Higgs physics,” *Z. Phys.* **C69** (1995) 77–88, [arXiv:hep-ph/9505225 \[hep-ph\]](#).
- [57] H. M. Georgi, S. L. Glashow, M. E. Machacek, and D. V. Nanopoulos, “Higgs Bosons from Two Gluon Annihilation in Proton Proton Collisions,” *Phys. Rev. Lett.* **40** (1978) 692.
- [58] J. R. Ellis, M. K. Gaillard, D. V. Nanopoulos, and C. T. Sachrajda, “Is the Mass of the Higgs Boson About 10-GeV?,” *Phys. Lett.* **83B** (1979) 339–344.
- [59] A. Denner, S. Heinemeyer, I. Puljak, D. Rebuffi, and M. Spira, “Standard Model Higgs-Boson Branching Ratios with Uncertainties,” *Eur. Phys. J.* **C71** (2011) 1753, [arXiv:1107.5909 \[hep-ph\]](#).
- [60] S. Goria, G. Passarino, and D. Rosco, “The Higgs Boson Lineshape,” *Nucl. Phys.* **B864** (2012) 530–579, [arXiv:1112.5517 \[hep-ph\]](#).
- [61] J. Campbell, J. Huston, and F. Krauss, *The Black Book of Quantum Chromodynamics*. Oxford University Press, 2017. <https://global.oup.com/academic/product/the-black-book-of-quantum-chromodynamics-9780199652747>.

- [62] J. Alwall, R. Frederix, S. Frixione, V. Hirschi, F. Maltoni, O. Mattelaer, H. S. Shao, T. Stelzer, P. Torrielli, and M. Zaro, “The automated computation of tree-level and next-to-leading order differential cross sections, and their matching to parton shower simulations,” *JHEP* **07** (2014) 079, [arXiv:1405.0301 \[hep-ph\]](#).
- [63] T. Gleisberg, S. Hoeche, F. Krauss, M. Schonherr, S. Schumann, F. Siegert, and J. Winter, “Event generation with SHERPA 1.1” *JHEP* **02** (2009) 007, [arXiv:0811.4622 \[hep-ph\]](#).
- [64] M. Bahr *et al.*, “Herwig++ Physics and Manual,” *Eur. Phys. J.* **C58** (2008) 639–707, [arXiv:0803.0883 \[hep-ph\]](#).
- [65] W. Kilian, T. Ohl, and J. Reuter, “WHIZARD: Simulating Multi-Particle Processes at LHC and ILC,” *Eur. Phys. J.* **C71** (2011) 1742, [arXiv:0708.4233 \[hep-ph\]](#).
- [66] **LHC Higgs Cross Section Working Group** Collaboration, D. de Florian *et al.*, “Handbook of LHC Higgs Cross Sections: 4. Deciphering the Nature of the Higgs Sector,” [arXiv:1610.07922 \[hep-ph\]](#).
- [67] C. Anastasiou, C. Duhr, F. Dulat, F. Herzog, and B. Mistlberger, “Higgs Boson Gluon-Fusion Production in QCD at Three Loops,” *Phys. Rev. Lett.* **114** (2015) 212001, [arXiv:1503.06056 \[hep-ph\]](#).
- [68] R. N. Cahn and S. Dawson, “Production of Very Massive Higgs Bosons,” *Phys. Lett.* **136B** (1984) 196. [Erratum: *Phys. Lett.* 138B,464(1984)].
- [69] D. L. Rainwater and D. Zeppenfeld, “Searching for  $H \rightarrow \gamma\gamma$  in weak boson fusion at the LHC,” *JHEP* **12** (1997) 005, [arXiv:hep-ph/9712271 \[hep-ph\]](#).
- [70] D. L. Rainwater, D. Zeppenfeld, and K. Hagiwara, “Searching for  $H \rightarrow \tau^+\tau^-$  in weak boson fusion at the CERN LHC,” *Phys. Rev.* **D59** (1998) 014037, [arXiv:hep-ph/9808468 \[hep-ph\]](#).
- [71] D. L. Rainwater and D. Zeppenfeld, “Observing  $H \rightarrow W^*W^* \rightarrow e^\pm\mu^\mp \cancel{p}_T$  in weak boson fusion with dual forward jet tagging at the CERN LHC,” *Phys. Rev.* **D60** (1999) 113004, [arXiv:hep-ph/9906218 \[hep-ph\]](#). [Erratum: *Phys. Rev.* D61,099901(2000)].
- [72] C. Englert, P. Harris, M. Spannowsky, and M. Takeuchi, “Unitarity-controlled resonances after the Higgs boson discovery,” *Phys. Rev.* **D92** no.~1, (2015) 013003, [arXiv:1503.07459 \[hep-ph\]](#).
- [73] S. Dawson, “The Effective W Approximation,” *Nucl. Phys.* **B249** (1985) 42–60.
- [74] T. Figy, C. Oleari, and D. Zeppenfeld, “Next-to-leading order jet distributions for Higgs boson production via weak boson fusion,” *Phys. Rev.* **D68** (2003) 073005, [arXiv:hep-ph/0306109 \[hep-ph\]](#).
- [75] B. Jager, C. Oleari, and D. Zeppenfeld, “Next-to-leading order QCD corrections to Z boson pair production via vector-boson fusion,” *Phys. Rev.* **D73** (2006) 113006, [arXiv:hep-ph/0604200 \[hep-ph\]](#).
- [76] B. Jager, C. Oleari, and D. Zeppenfeld, “Next-to-leading order QCD corrections to W+W-production via vector-boson fusion,” *JHEP* **07** (2006) 015, [arXiv:hep-ph/0603177 \[hep-ph\]](#).
- [77] P. Bolzoni, F. Maltoni, S.-O. Moch, and M. Zaro, “Vector boson fusion at NNLO in QCD: SM Higgs and beyond,” *Phys. Rev.* **D85** (2012) 035002, [arXiv:1109.3717 \[hep-ph\]](#).

- [78] M. Cacciari, F. A. Dreyer, A. Karlberg, G. P. Salam, and G. Zanderighi, “Fully Differential Vector-Boson-Fusion Higgs Production at Next-to-Next-to-Leading Order,” *Phys. Rev. Lett.* **115** no.-8, (2015) 082002, [arXiv:1506.02660 \[hep-ph\]](#). [Erratum: *Phys. Rev. Lett.* 120,no.13,139901(2018)].
- [79] M. Ciccolini, A. Denner, and S. Dittmaier, “Strong and electroweak corrections to the production of Higgs + 2jets via weak interactions at the LHC,” *Phys. Rev. Lett.* **99** (2007) 161803, [arXiv:0707.0381 \[hep-ph\]](#).
- [80] M. Ciccolini, A. Denner, and S. Dittmaier, “Electroweak and QCD corrections to Higgs production via vector-boson fusion at the LHC,” *Phys. Rev.* **D77** (2008) 013002, [arXiv:0710.4749 \[hep-ph\]](#).
- [81] V. D. Barger, K.-m. Cheung, T. Han, and D. Zeppenfeld, “Single forward jet tagging and central jet vetoing to identify the leptonic  $WW$  decay mode of a heavy Higgs boson,” *Phys. Rev.* **D44** (1991) 2701. [Erratum: *Phys. Rev.* D48,5444(1993)].
- [82] V. D. Barger, R. J. N. Phillips, and D. Zeppenfeld, “Mini - jet veto: A Tool for the heavy Higgs search at the LHC,” *Phys. Lett.* **B346** (1995) 106–114, [arXiv:hep-ph/9412276 \[hep-ph\]](#).
- [83] O. J. P. Eboli and D. Zeppenfeld, “Observing an invisible Higgs boson,” *Phys. Lett.* **B495** (2000) 147–154, [arXiv:hep-ph/0009158 \[hep-ph\]](#).
- [84] J. M. Campbell, R. K. Ellis, and C. Williams, “Associated production of a Higgs boson at NNLO,” *JHEP* **06** (2016) 179, [arXiv:1601.00658 \[hep-ph\]](#).
- [85] J. M. Butterworth, A. R. Davison, M. Rubin, and G. P. Salam, “Jet substructure as a new Higgs search channel at the LHC,” *Phys. Rev. Lett.* **100** (2008) 242001, [arXiv:0802.2470 \[hep-ph\]](#).
- [86] S. Marzani, G. Soyez, and M. Spannowsky, “Looking inside jets: an introduction to jet substructure and boosted-object phenomenology,” [arXiv:1901.10342 \[hep-ph\]](#).
- [87] L. Reina and S. Dawson, “Next-to-leading order results for  $t$  anti- $t$   $h$  production at the Tevatron,” *Phys. Rev. Lett.* **87** (2001) 201804, [arXiv:hep-ph/0107101 \[hep-ph\]](#).
- [88] L. Reina, S. Dawson, and D. Wackerroth, “QCD corrections to associated  $t$  anti- $t$   $h$  production at the Tevatron,” *Phys. Rev.* **D65** (2002) 053017, [arXiv:hep-ph/0109066 \[hep-ph\]](#).
- [89] S. Dawson, L. H. Orr, L. Reina, and D. Wackerroth, “Associated top quark Higgs boson production at the LHC,” *Phys. Rev.* **D67** (2003) 071503, [arXiv:hep-ph/0211438 \[hep-ph\]](#).
- [90] S. Dawson, C. Jackson, L. H. Orr, L. Reina, and D. Wackerroth, “Associated Higgs production with top quarks at the large hadron collider: NLO QCD corrections,” *Phys. Rev.* **D68** (2003) 034022, [arXiv:hep-ph/0305087 \[hep-ph\]](#).
- [91] W. Beenakker, S. Dittmaier, M. Kramer, B. Plumper, M. Spira, and P. M. Zerwas, “Higgs radiation off top quarks at the Tevatron and the LHC,” *Phys. Rev. Lett.* **87** (2001) 201805, [arXiv:hep-ph/0107081 \[hep-ph\]](#).
- [92] W. Beenakker, S. Dittmaier, M. Kramer, B. Plumper, M. Spira, and P. M. Zerwas, “NLO QCD corrections to  $t$  anti- $t$   $H$  production in hadron collisions,” *Nucl. Phys.* **B653** (2003) 151–203, [arXiv:hep-ph/0211352 \[hep-ph\]](#).
- [93] A. Denner, S. Dittmaier, S. Kallweit, and S. Pozzorini, “NLO QCD corrections to off-shell top-antitop production with leptonic decays at hadron colliders,” *JHEP* **10** (2012) 110, [arXiv:1207.5018 \[hep-ph\]](#).

- [94] A. Denner, J.-N. Lang, M. Pellen, and S. Uccirati, “Higgs production in association with off-shell top-antitop pairs at NLO EW and QCD at the LHC,” *JHEP* **02** (2017) 053, arXiv:1612.07138 [hep-ph].
- [95] ATLAS Collaboration, A. Airapetian *et al.*, “ATLAS: Detector and physics performance technical design report. Volume 2,” CERN-LHCC-99-15, ATLAS-TDR-15.
- [96] J. Cammin and M. Schumacher, “The ATLAS discovery potential for the channel ttH, H to bb,” ATL-PHYS-2003-024, ATL-COM-PHYS-2003-027, CERN-ATL-PHYS-2003-024.
- [97] T. Plehn, G. P. Salam, and M. Spannowsky, “Fat Jets for a Light Higgs,” *Phys. Rev. Lett.* **104** (2010) 111801, arXiv:0910.5472 [hep-ph].
- [98] T. Plehn and M. Spannowsky, “Top Tagging,” *J. Phys.* **G39** (2012) 083001, arXiv:1112.4441 [hep-ph].
- [99] CMS Collaboration, A. M. Sirunyan *et al.*, “Observation of ttH production,” arXiv:1804.02610 [hep-ex].
- [100] ATLAS Collaboration, M. Aaboud *et al.*, “Observation of Higgs boson production in association with a top quark pair at the LHC with the ATLAS detector,” arXiv:1806.00425 [hep-ex].
- [101] CMS Collaboration, A. M. Sirunyan *et al.*, “Observation of Higgs boson decay to bottom quarks,” *Phys. Rev. Lett.* **121** no.~12, (2018) 121801, arXiv:1808.08242 [hep-ex].
- [102] ATLAS Collaboration, M. Aaboud *et al.*, “Observation of  $H \rightarrow b\bar{b}$  decays and VH production with the ATLAS detector,” *Phys. Lett.* **B786** (2018) 59–86, arXiv:1808.08238 [hep-ex].
- [103] ATLAS Collaboration, T. A. collaboration, “Combined measurements of Higgs boson production and decay using up to 80 fb<sup>-1</sup> of proton–proton collision data at  $\sqrt{s} = 13$  TeV collected with the ATLAS experiment,”.
- [104] C. Englert, M. McCullough, and M. Spannowsky, “Gluon-initiated associated production boosts Higgs physics,” *Phys. Rev.* **D89** no.~1, (2014) 013013, arXiv:1310.4828 [hep-ph].
- [105] R. V. Harlander, S. Liebler, and T. Zirke, “Higgs Strahlung at the Large Hadron Collider in the 2-Higgs-Doublet Model,” *JHEP* **02** (2014) 023, arXiv:1307.8122 [hep-ph].
- [106] A. J. Barr, M. J. Dolan, C. Englert, D. E. Ferreira de Lima, and M. Spannowsky, “Higgs Self-Coupling Measurements at a 100 TeV Hadron Collider,” *JHEP* **02** (2015) 016, arXiv:1412.7154 [hep-ph].
- [107] U. Baur, T. Plehn, and D. L. Rainwater, “Determining the Higgs Boson Selfcoupling at Hadron Colliders,” *Phys. Rev.* **D67** (2003) 033003, arXiv:hep-ph/0211224 [hep-ph].
- [108] U. Baur, T. Plehn, and D. L. Rainwater, “Measuring the Higgs boson self coupling at the LHC and finite top mass matrix elements,” *Phys. Rev. Lett.* **89** (2002) 151801, arXiv:hep-ph/0206024 [hep-ph].
- [109] U. Baur, T. Plehn, and D. L. Rainwater, “Probing the Higgs selfcoupling at hadron colliders using rare decays,” *Phys. Rev.* **D69** (2004) 053004, arXiv:hep-ph/0310056 [hep-ph].
- [110] U. Baur, T. Plehn, and D. L. Rainwater, “Examining the Higgs boson potential at lepton and hadron colliders: A Comparative analysis,” *Phys. Rev.* **D68** (2003) 033001, arXiv:hep-ph/0304015 [hep-ph].
- [111] M. J. Dolan, C. Englert, and M. Spannowsky, “Higgs self-coupling measurements at the LHC,” *JHEP* **10** (2012) 112, arXiv:1206.5001 [hep-ph].

- [112] D. E. Ferreira de Lima, A. Papaefstathiou, and M. Spannowsky, “Standard model Higgs boson pair production in the  $(b\bar{b})(b\bar{b})$  final state,” *JHEP* **08** (2014) 030, arXiv:1404.7139 [hep-ph].
- [113] R. Contino *et al.*, “Physics at a 100 TeV pp collider: Higgs and EW symmetry breaking studies,” *CERN Yellow Report* no.~3, (2017) 255–440, arXiv:1606.09408 [hep-ph].
- [114] H. E. Logan, “TASI 2013 lectures on Higgs physics within and beyond the Standard Model,” arXiv:1406.1786 [hep-ph].
- [115] M. Buschmann, D. Goncalves, S. Kuttimalai, M. Schonherr, F. Krauss, and T. Plehn, “Mass Effects in the Higgs-Gluon Coupling: Boosted vs Off-Shell Production,” *JHEP* **02** (2015) 038, arXiv:1410.5806 [hep-ph].
- [116] T. Corbett, O. J. P. Eboli, D. Goncalves, J. Gonzalez-Fraile, T. Plehn, and M. Rauch, “The Higgs Legacy of the LHC Run I,” *JHEP* **08** (2015) 156, arXiv:1505.05516 [hep-ph].
- [117] A. Biekutter, D. Gonalves, T. Plehn, M. Takeuchi, and D. Zerwas, “The Global Higgs Picture at 27 TeV,” arXiv:1811.08401 [hep-ph].
- [118] J. Ellis, C. W. Murphy, V. Sanz, and T. You, “Updated Global SMEFT Fit to Higgs, Diboson and Electroweak Data,” arXiv:1803.03252 [hep-ph].
- [119] G. F. Giudice, C. Grojean, A. Pomarol, and R. Rattazzi, “The Strongly-Interacting Light Higgs,” *JHEP* **06** (2007) 045, arXiv:hep-ph/0703164 [hep-ph].
- [120] C. Englert, R. Kogler, H. Schulz, and M. Spannowsky, “Higgs characterisation in the presence of theoretical uncertainties and invisible decays,” *Eur. Phys. J.* **C77** no.~11, (2017) 789, arXiv:1708.06355 [hep-ph].
- [121] F. Caola, S. Forte, S. Marzani, C. Muselli, and G. Vita, “The Higgs transverse momentum spectrum with finite quark masses beyond leading order,” *JHEP* **08** (2016) 150, arXiv:1606.04100 [hep-ph].
- [122] J. Brehmer, K. Cranmer, F. Kling, and T. Plehn, “Better Higgs boson measurements through information geometry,” *Phys. Rev.* **D95** no.~7, (2017) 073002, arXiv:1612.05261 [hep-ph].
- [123] C. Grojean, E. E. Jenkins, A. V. Manohar, and M. Trott, “Renormalization Group Scaling of Higgs Operators and  $\Gamma(h \rightarrow \gamma\gamma)$ ,” *JHEP* **04** (2013) 016, arXiv:1301.2588 [hep-ph].
- [124] R. Alonso, E. E. Jenkins, A. V. Manohar, and M. Trott, “Renormalization Group Evolution of the Standard Model Dimension Six Operators III: Gauge Coupling Dependence and Phenomenology,” *JHEP* **04** (2014) 159, arXiv:1312.2014 [hep-ph].
- [125] E. E. Jenkins, A. V. Manohar, and M. Trott, “Renormalization Group Evolution of the Standard Model Dimension Six Operators II: Yukawa Dependence,” *JHEP* **01** (2014) 035, arXiv:1310.4838 [hep-ph].
- [126] E. E. Jenkins, A. V. Manohar, and M. Trott, “Renormalization Group Evolution of the Standard Model Dimension Six Operators I: Formalism and lambda Dependence,” *JHEP* **10** (2013) 087, arXiv:1308.2627 [hep-ph].
- [127] C. Englert and M. Spannowsky, “Effective Theories and Measurements at Colliders,” *Phys. Lett.* **B740** (2015) 8–15, arXiv:1408.5147 [hep-ph].